

Journal of Materials Chemistry A

Materials for energy and sustainability

Accepted Manuscript

This article can be cited before page numbers have been issued, to do this please use: D. Lu and H. Chen, *J. Mater. Chem. A*, 2024, DOI: 10.1039/D4TA05288A.



This is an Accepted Manuscript, which has been through the Royal Society of Chemistry peer review process and has been accepted for publication.

Accepted Manuscripts are published online shortly after acceptance, before technical editing, formatting and proof reading. Using this free service, authors can make their results available to the community, in citable form, before we publish the edited article. We will replace this Accepted Manuscript with the edited and formatted Advance Article as soon as it is available.

You can find more information about Accepted Manuscripts in the [Information for Authors](#).

Please note that technical editing may introduce minor changes to the text and/or graphics, which may alter content. The journal's standard [Terms & Conditions](#) and the [Ethical guidelines](#) still apply. In no event shall the Royal Society of Chemistry be held responsible for any errors or omissions in this Accepted Manuscript or any consequences arising from the use of any information it contains.

1 **Solid-State Organic Electrochemical Transistors (OECT) Based on**
2 **Gel Electrolytes for Biosensors and Bioelectronics**

3 Dongdong Lu^{a*}, Hu Chen^{a*}

4 a. Dongguan Key Laboratory of Interdisciplinary Science for Advanced Materials and
5 Large-Scale Scientific Facilities, School of Physical Sciences, Great Bay University,
6 Dongguan, Guangdong, 523000, P. R. China

7 E-mail: ludongdong@gbu.edu.cn

8 E-mail: chenhu@gbu.edu.cn



1 **Abstract**

View Article Online
DOI: 10.1039/D4TA05288A

2 Organic electrochemical transistor (OECT) have emerged as promising platforms for
3 biosensors and bioelectronic devices due to their biocompatibility, low power
4 consumption, and sensitivity in amplifying chemical signals. This review delves into
5 the recent advancements in the field of biosensors and bioelectronics utilizing solid-
6 state OECT with flexible gel electrolytes. Gel electrolytes, including hydrogels and
7 ionic liquid gels, offer improved mechanical compatibility and stability compared to
8 traditional liquid electrolytes, making them suitable for wearable and implantable
9 biosensing applications. We explore the properties and classifications of gel
10 electrolytes for OECT, highlighting their self-healing, responsive, temperature-resistant,
11 adhesive, and stretchable characteristics. Moreover, we discuss the application of solid-
12 state OECT based on gel electrolytes in ion sensing, metabolite detection, and
13 electrophysiological sensing. Despite significant progress, challenges such as
14 manufacturing scalability and the development of responsive OECT persist. Future
15 directions involve leveraging the multi-responsiveness of hydrogel electrolytes for
16 intelligent sensor designs, integrating solid-state OECT with energy storage devices for
17 self-powered applications, and advancing wireless communication functionalities for
18 real-time health monitoring. This comprehensive overview provides insights into the
19 potential of solid-state OECT based on gel electrolytes and outlines future research
20 directions in biosensing and bioelectronics.



1 1. Introduction of OEET

2 Owing to their biocompatible nature, low energy consumption, and minimal operational
3 voltage, organic electrochemical transistor (OEET) have become highly regarded as
4 potential options for advancing biosensors and bioelectronic devices¹⁻⁴. OEET exhibit
5 high transconductance, facilitating sensitive amplification of chemical signals, thus
6 holding significant potential across various biomedical applications, including ion
7 sensing⁵⁻⁶, DNA detection⁷, alcohol sensing⁸, metabolite detection⁹, and cell
8 detection¹⁰⁻¹¹. Traditional OEETs consist of three-terminal devices with source, drain,
9 and gate electrodes¹². An organic semiconductor layer serves as a conducting channel,
10 isolated from the gate electrode by an ion-conducting electrolyte. OEET operation
11 relies on interplay between ion and charge transport, resulting in modulation of the
12 current (I_{DS}) flowing from source to drain through the conducting channel¹. The
13 transconductance parameter (g_m) evaluates the amplification characteristics of OEETs,
14 crucial for enhancing sensing performance, characterized by the detection limit (LOD,
15 signal-to-noise ratio ≥ 3)¹³⁻¹⁴.

$$16 \quad g_m = \frac{\partial I_D}{\partial V_G} = \frac{Wd}{L} \mu_n C^* (V_{th} - V_G) \quad \text{Equation (1)}$$

17 In the equation, W , L , and d denote the channel width, length, and thickness,
18 respectively; μ , C^* , and V_{th} are the carrier mobility, volume capacitance, and threshold
19 voltage of the active layer, respectively. High-performance OEET can be achieved by
20 optimizing the geometry of devices based on Organic Mixed Ionic-Electronic
21 Conductor (OMIEC) or μC^* values¹⁵⁻¹⁶, as indicated by Equation (1)¹⁷⁻¹⁸.

22 Currently, research on OEET predominantly center on the study of active materials,
23 electrolytes, interface modification, and the optimization of device geometry.
24 Enhancing electronic properties of OMIEC, such as high mobility and large capacitance,
25 is crucial for achieving high-performance OEET^{17, 19}. Notably, poly(3,4-
26 ethylenedioxythiophene)-poly(styrene sulfonate) (PEDOT:PSS) has exhibited a



1 maximum μC^* product of $1500 \text{ F cm}^{-1} \text{ V}^{-1} \text{ s}^{-1}$ due to its exceptional conductivity
2 properties¹⁷. This achievement is based on the original hole current of PEDOT:PSS of
3 OECT reaching its maximum value at zero gate bias. When applying a positive gate
4 voltage, cations (e.g., Na^+ , K^+ , and Li^+) from the electrolyte move into the organic
5 channel, leading to de-doping of PEDOT through electrochemical reactions as shown
6 in Equation (2). As highly conductive PEDOT^+ is reduced to non-conductive PEDOT^0 ,
7 the device's drain current decreases, demonstrating typical depletion-mode transistor
8 behavior¹⁶. Additionally, multifunctional OECT employ various strategies, including
9 interface modification and functional materials, to modulate the OECT ion circuit and
10 manipulate charge transport within the channel²⁰⁻²¹.



12 While liquid electrolyte-based OECT have been prevalent, their liquid nature presents
13 challenges such as leakage, evaporation, environmental contamination and electrolyte
14 electrolysis, hindering long-term stability and performance²²⁻²⁴. To address these issues,
15 solid-state OECT have emerged as a promising alternative, particularly suitable for
16 wearable biosensing and flexible electronic applications²⁵⁻²⁷. Solid-state electrolytes
17 facilitate large-scale manufacturing of compact and highly integrated OECT using
18 simple printing techniques²⁸. Moreover, they provide superior flexibility and
19 durability²⁷ by enabling the devices to withstand daily wear and mechanical stresses²⁹⁻
20 ³⁰.

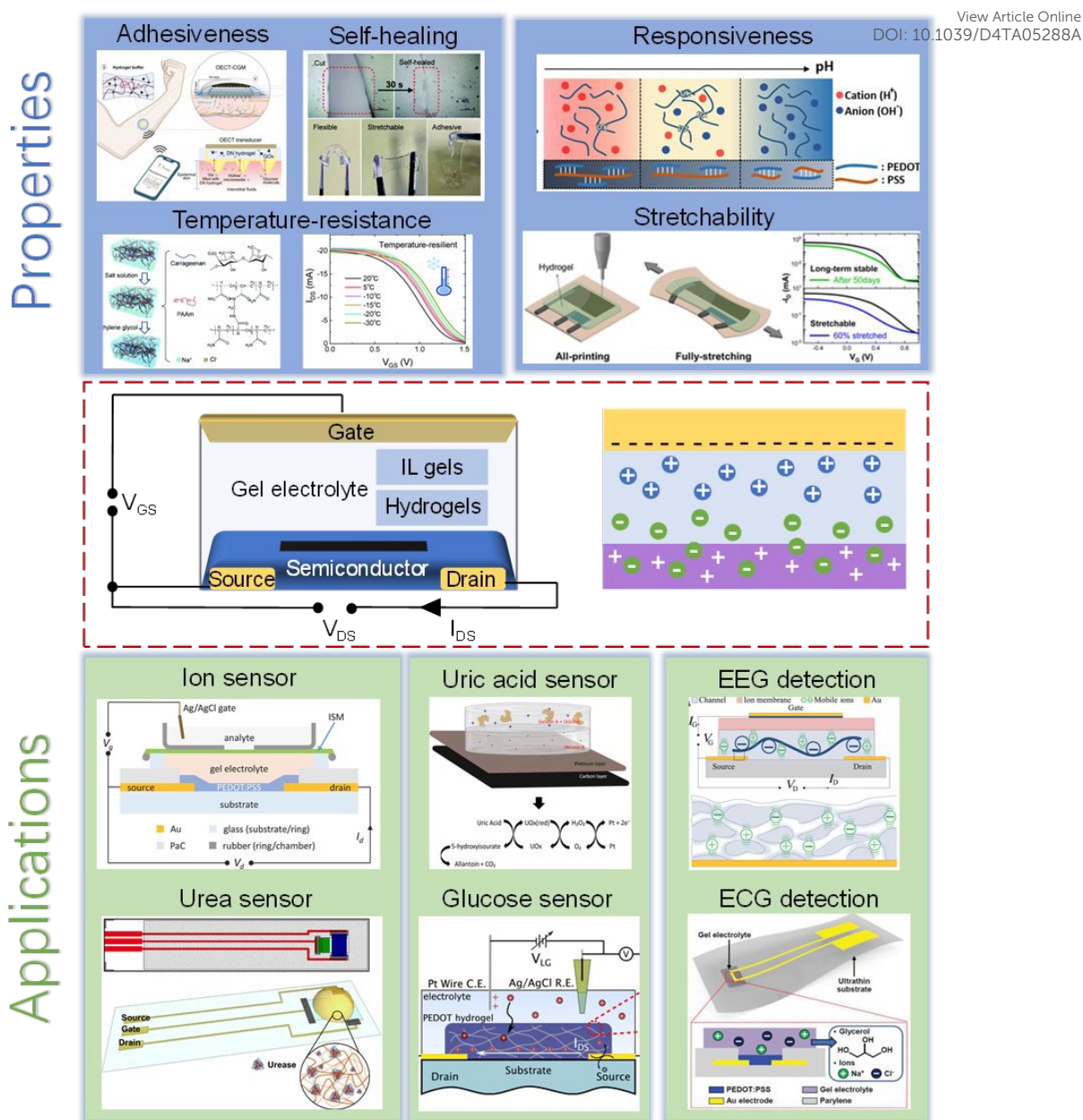
21 **2. Gel-electrode**

22 Gels, characterized by cross-linked three-dimensional polymer networks, possess a
23 unique ability to swell in liquid electrolytes, effectively absorbing and immobilizing
24 them. This distinctive property combines the high ion conductivity of liquid electrolytes
25 with the processability of solid electrolytes, thereby addressing concerns related to
26 liquid leakage. Furthermore, the high hydration capacity of gels facilitates ion transport,



1 ensuring compatibility with biological tissues³¹. Notably, their mechanical properties
2 closely resemble those of human tissues, with Young's modulus ranging from 1 Pa to
3 300 MPa, covering the ranges of skin and muscle (200–500 kPa) and brain tissue and
4 spinal cord (500 Pa–200 kPa)³². This mechanical compatibility with soft tissues makes
5 hydrogels an ideal choice for implants and wearable bioelectronics³³. The gel
6 electrolytes utilized in OECT are typically classified into two categories: hydrogels and
7 ionic liquid gels (IL gels). This review specifically hones in on the classification and
8 properties of gel electrolytes, and summarizes the progress of gel electrolyte-based
9 OECT applications in the fields of biosensing and bioelectronics (**Figure 1**).
10 Furthermore, the review provides an overview of the existing challenges encountered
11 in this field and proposes future research directions to address them effectively.





1
2 **Figure 1.** Schematic illustration of the advancement of gel electrolyte-based OECT in
3 terms of their characteristics and diverse applications. Reproduced from Ref.³⁴⁻⁴⁴;
4 Copyright 2020, American Chemical Society³⁵; Copyright 2018, American Chemical
5 Society³⁷; Copyright 2021, American Chemical Society³⁶; Copyright 2024, AAAS ³⁴;
6 Copyright 2023, Royal Society of Chemistry³⁸; Copyright 2014, Wiley-VCH³⁹;
7 Copyright 2018, IOP publishing, Ltd⁴⁰; Copyright 2020, Wiley-VCH⁴¹; Copyright 2022,
8 American Chemical Society⁴²; Copyright 2019, AAAS⁴³; Copyright 2019, Wiley-
9 VCH⁴⁴.



1 2.1 Categories of gel-electrodes

2 2.1.1 Hydrogels

3 Hydrogels, characterized by their three-dimensional cross-linked polymer networks,
4 offer a versatile platform with tunable physicochemical properties such as
5 biocompatibility, biodegradability, material transport, and mechanical strength⁴⁵. These
6 properties make them conducive to loading and delivering cells, drugs and growth
7 factors, thereby facilitating cell adhesion and proliferation⁴⁶⁻⁴⁸. Hydrogels primarily
8 conduct protons, with ion transport facilitated by the diffusion of intramolecular and
9 intermolecular hydrogen bonds within the polymer matrix or residual free volume
10 water⁴⁹. Studies have demonstrated that increasing glycerol concentration can enhance
11 hydrogel ion conductivity⁵⁰⁻⁵¹. Consequently, solid-state OECT employing various
12 hydrogel electrolytes have been developed for applications in biosensing⁴¹, synaptic
13 neural simulation⁵², and bioelectronics⁵³. Examples of synthesized hydrogel
14 electrolytes include poly(ethylene glycol) (PEG)⁵⁴, poly(N-isopropylacrylamide)
15 (PNIPAm)⁵⁵, poly(hydroxyethyl acrylate) (PHEA)⁵⁶, poly(hydroxyethyl methacrylate)
16 (PHEMA)⁵⁷, and poly(vinyl alcohol) (PVA)³⁸. These hydrogels offer excellent
17 controllability, ease of design, and mechanical properties that can be tailored to mimic
18 natural tissues, thereby reducing interface resistance and enhancing compliance with
19 biological systems.

20 Natural hydrogels, including gelatin³⁷, chitosan⁴³, agar, etc, derived from biomaterials
21 offer distinct advantages over synthetic counterparts, including inherent
22 biocompatibility, low cytotoxicity, and environmental friendliness. However, they may
23 exhibit weaker mechanical structures and susceptibility to degradation. It is imperative
24 to maintain precise control over the molecular weight and composition of the polymer
25 in order to align with the specific demands of solid-state OECT, including
26 biomechanical properties and gel behavior. Composite hydrogels, combine natural and



1 synthetic materials, offer enhanced mechanical properties and biocompatibility,
2 presenting promising avenues for future research. For example, Liu et al. reported
3 OECTs based on a dual-network antifreeze hydrogel, comprising cross-linked
4 polyacrylamide (PAAm) and carrageenan. This innovative hydrogel demonstrated
5 remarkable attributes including biocompatibility, mechanical strength, antifreeze
6 properties, and high ion conductivity, enabling operation at $-30\text{ }^{\circ}\text{C}$ ^{36, 58}. However, the
7 preparation methods for these hydrogel electrolytes commonly involve swelling in salt
8 solutions (e.g., sodium chloride) or phosphate-buffered saline) to enhance ion
9 conductivity. Nevertheless, this structure is susceptible to deformation at elevated
10 temperatures and prolonged use. Moreover, water evaporation can diminish the free
11 volume conduction path of ions, resulting in leading to performance degradation in
12 hydrogel-based OECTs.

13 **2.1.2 Ionic liquid gels**

14 Ionic liquid gels (IL gels), comprising non-volatile ionic liquids with low melting points
15 below $100\text{ }^{\circ}\text{C}$, have emerged as an alternative to hydrogels, particularly for flexible
16 electronic devices⁵⁹, biosensors⁶⁰⁻⁶¹ and solid-state OECT⁶². IL gels offer advantages
17 such as minimal vapor pressure, high thermal stability, and superior ionic conductivity⁶³.
18 Numerous studies have delved into the synthesis of ionic gels, elucidating ion transport
19 mechanisms and the dynamics of ion/electron interface transport⁶⁴. These
20 investigations have significantly enhanced the understanding of ionic gels across
21 various relevant fields⁶⁵⁻⁶⁶. Common ionic liquids used in IL gels include 1-ethyl-3-
22 methylimidazolium ethylsulfate ($[\text{C}_2\text{MIM}][\text{EtSO}_4]$), 1-butyl-3-methylimidazolium
23 bis(trifluoromethylsulfonyl)imide ($[\text{BMIM}][\text{TFSI}]$), and 1-ethyl-3-methylimidazolium
24 bis(trifluoromethylsulfonyl)imide ($[\text{EMIM}][\text{TFSI}]$). However, their toxicity and high
25 fluoride content limit direct contact with skin and the environment^{55, 67}. Biocompatible
26 ILs containing choline cations and amino acids or carboxylic acids as anions (e.g.,
27 choline lactate ($[\text{Ch}][\text{Lac}]$) or choline glycolate ($[\text{Ch}][\text{Glyco}]$)) have been developed⁶⁸⁻



1 ⁶⁹, offering high ionic conductivity, biocompatibility, and environmental stability⁷⁰⁻⁷¹.
2 These materials hold promise for implementing all-solid-state OECT in long-term
3 biomedical applications such as skin electrophysiology monitoring.

4 **2.2 Properties of gel electrolyte**

5 The unique properties and advantages of gel electrolytes grant OECT several critical
6 functionalities. Hydrogels have highly tunable physical and chemical properties. Their
7 conductivity, mechanical strength, and biocompatibility can be precisely controlled by
8 altering their composition and structure⁷²⁻⁷³. This tunability allows OECT to meet
9 various application requirements, enabling highly customized sensor designs. Due to
10 their softness, gel electrolytes combined with OECT can achieve greater mechanical
11 flexibility and stability⁷⁴, making them ideal for wearable and implantable applications.
12 The high-water content of hydrogels provides exceptional ionic conductivity, allowing
13 OECT to operate efficiently at low voltages, enhancing electrochemical conversion
14 efficiency and signal amplification¹¹. The biocompatibility of hydrogels makes them
15 particularly suitable for biomedical applications in OECT. Hydrogels are not only
16 compatible with biological tissues but also maintain stability in in vivo environments⁷⁵,
17 reducing potential irritation and immune responses⁷⁶. This characteristic allows OECT
18 to play vital roles in real-time biosignal monitoring, drug delivery control, and
19 implantable medical devices. Moreover, specially designed smart responsive and
20 thermally stable hydrogel electrolytes can expand the application range of OECT^{36, 77-}
21 ⁷⁸. Responsive hydrogel electrolytes allow OECT to quickly adjust their
22 electrochemical properties to changes in the external environment, achieving high-
23 sensitivity and rapid-response sensing applications. Thermally stable hydrogels
24 maintain their structural and functional integrity under high or low temperatures,
25 ensuring consistent operation. This thermal stability ensures that OECT maintain their
26 performance under various environmental conditions, preventing degradation or failure
27 due to temperature fluctuations. This characteristic is particularly advantageous for



1 biomedical devices and sensors operating in complex environments. This chapter
2 discusses the research progress of solid-state OECT based on gel electrolytes from the
3 perspectives of conductivity and volumetric capacitance, self-healing, stretchability,
4 responsiveness, temperature-resistance, and self-adhesion.

5 **2.2.1 Conductivity and volumetric capacitance**

6 In Equation 1, as introduced in the OECT discussion, the parameter μC^* represents a
7 key intrinsic property of OECT. In this expression, μ denotes the charge carrier mobility,
8 a measure of how easily charges move through the material, while C^* stands for the
9 volumetric capacitance, which reflects the ability of the material to store charges per
10 unit volume. Together, the μC^* product determines the overall transconductance and
11 performance of the OECT, influencing the sensitivity and amplification of the device
12 in biosensing applications. The μC^* value is a fundamental factor in the design and
13 optimization of OECT, as it directly relates to the efficiency of ion-electron coupling
14 and signal transduction within the device. By maximizing both the mobility (μ) and
15 capacitance (C^*), high-performance OECT can be achieved, which are essential for
16 applications requiring fast, sensitive detection and stable operation under low voltages.

17 Optimizing the μC^* value, therefore, is crucial for advancing the application of OECT
18 in bioelectronics, particularly in real-time health monitoring and biosensor technologies.

19 The extraction of electronic mobility in OFETs is well-established, but applying similar
20 techniques to OECT is challenging due to the presence of both ionic and electronic
21 charges in the OECT channel. Moreover, the mobility in OECT can be voltage-
22 dependent due to variations in electronic charge density across the film, resulting from
23 changes in the electrochemical potential from the source to the drain. At high doping
24 potentials, electronic charges can saturate available states (HOMO or LUMO), reducing
25 the efficiency of charge transport. To determine the capacitance of materials used in
26 OECT, electrochemical impedance spectroscopy (EIS) is frequently employed. The



1 typical EIS setup involves a three-electrode system, with the OMIEC film serving as
2 the working electrode, alongside a reference electrode and counter electrode. The
3 counter electrode must possess a significantly larger capacitance than the working
4 electrode to ensure it doesn't hinder the reactions occurring at the working electrode.
5 The process involves applying a small alternating current modulation across a range of
6 frequencies (typically from 10^6 to 10^{-1} Hz) on top of a direct current offset. Once the
7 impedance data is collected, capacitance (C) can be extracted, typically at lower
8 frequencies where ionic movement is slower and more capacitive behavior is observed.
9 Capacitance can also be derived through cyclic voltammetry. In the absence of faradaic
10 reactions, the voltammogram can be integrated to estimate the volumetric capacitance,
11 assuming ideal capacitor behavior in the OMIEC film. This method closely aligns with
12 the results from EIS.

13 However, if redox peaks are present, those areas are excluded to avoid skewing the
14 capacitance calculation. Additionally, it is important to consider factors like scan rate,
15 as overly fast scans may lead to underestimation of capacitance due to incomplete
16 charging/discharging cycles. Lastly, for accurate results, capacitance should be
17 measured for films of varying geometries, ensuring the extracted values scale linearly
18 with the film volume.

19 **2.2.2 Self-healing property**

20 Incorporating self-healing materials into solid-state OECT presents an intriguing
21 avenue for creating devices with enhanced reliability and prolonged lifespans. However,
22 the utilization of self-healing materials in OECT is currently in its nascent stages. One
23 of the primary challenges is to achieve effective repair performance while preserving
24 the electronic/ion transport and mechanical properties of both the conjugated polymer
25 and solid electrolyte, ensuring swift restoration to the original performance post-self-
26 healing.



1 Fabio Cicoira's work revealed that PEDOT:PSS thin films underwent rapid electrical
2 repair (approximately 150 ms) simply by wetting the damaged area with water⁷⁹.
3 Hydrogels, renowned for their self-healing properties, leverage dynamic bonding
4 interactions such as dynamic covalent bonds⁸⁰, hydrogen bonds⁸¹⁻⁸³, ion bonds⁸⁴,
5 supramolecular host-guest interactions⁸⁵, and hydrophobic interactions⁸⁶. In addition,
6 the high water content of the hydrogel can give PEDOT:PSS self-healing properties.
7 Wei Lin Leong et.al.³⁵ pioneered the development of a solid-state OECT endowed with
8 self-healing capabilities and robust electrical performance. Their design utilized a
9 PEDOT:PSS and surfactant Triton X-100 (PEDOT:PSS/TX) matrix as the channel,
10 coupled with an poly(vinyl alcohol) (PVA) hydrogel as the electrolyte. The high ionic
11 conductivity of the PVA hydrogel ($9.8 \times 10^{-3} \text{ S cm}^{-1}$) facilitated OECT operation by
12 modulating PEDOT:PSS doping. The resulting PEDOT:PSS/TX-PVA based OECT
13 exhibited impressive peak transconductance (48.7 mS) and on/off ratio (≈ 1500) (**Figure**
14 **2A**). The TX functions as both an enhancer of electrical performance and a self-
15 repairing agent. When the damaged area comes into contact with the PVA hydrogel,
16 it triggers both physical and electrical self-repair of the PEDOT:PSS/TX film (**Figure**
17 **2B**). Consequently, the OECT autonomously restored its initial performance to a range
18 of 85%-100% post-damage (**Figure 2C**), with a transconductance of approximately 45
19 mS at $V_G = -0.075 \text{ V}$ and an on/off ratio of ~ 1300 (**Figure 2D**). Additionally, as an ion
20 sensor, this OECT demonstrated the capability to detect Na^+ .



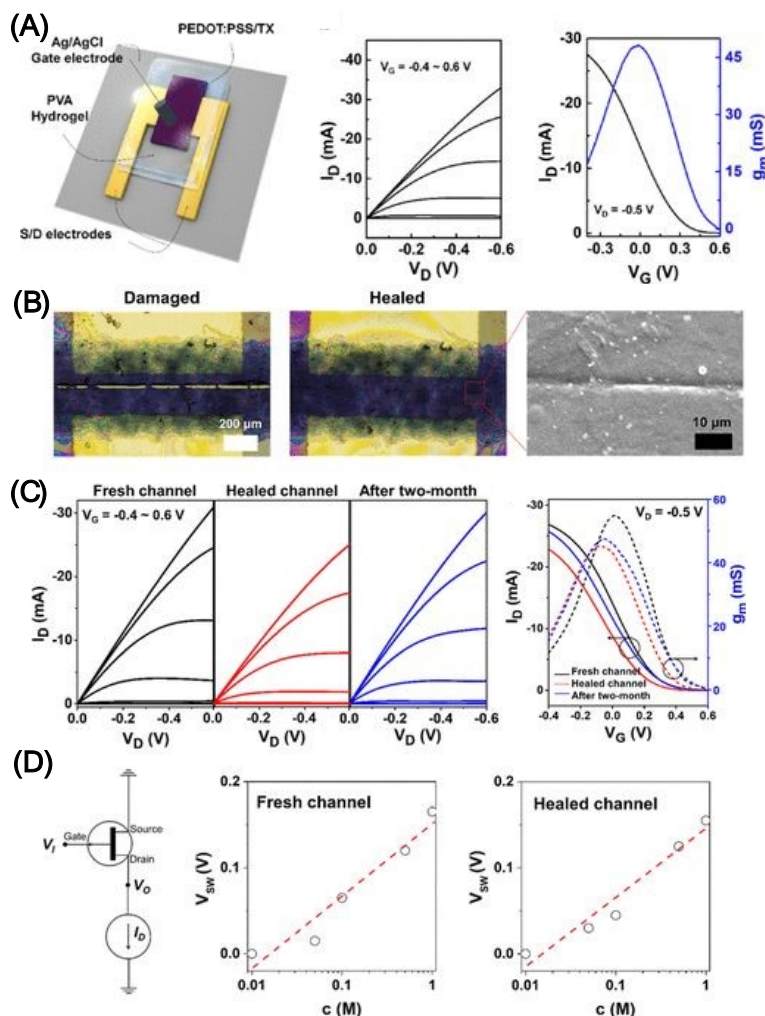


Figure 2. (A) Schematic diagram of the PEDOT:PSS/TX-PVA based OECT and its output and transfer characteristic. (B) Optical and SEM images depicting the structural characteristics of damaged and healed PEDOT:PSS/TX channel layers. (C) Output and transfer characteristic of OECT before and after self-healing. (D) Cumulative variation in switching voltage of the OECTs of ion concentration before damage and after healing. Reproduced with permission³⁵. Copyright 2020, American Chemical Society.

2.2.3 Responsiveness

Environmental stimulus responsiveness is a compelling attribute of hydrogels, as they can dynamically adjust their properties (such as water content, surface charge, hydrophilicity-hydrophobicity, and mechanical modulus) in response to various stimuli. These stimuli encompass chemical cues (e.g., pH⁸⁷, oxidizing agents⁸⁸, ions⁸⁹, and

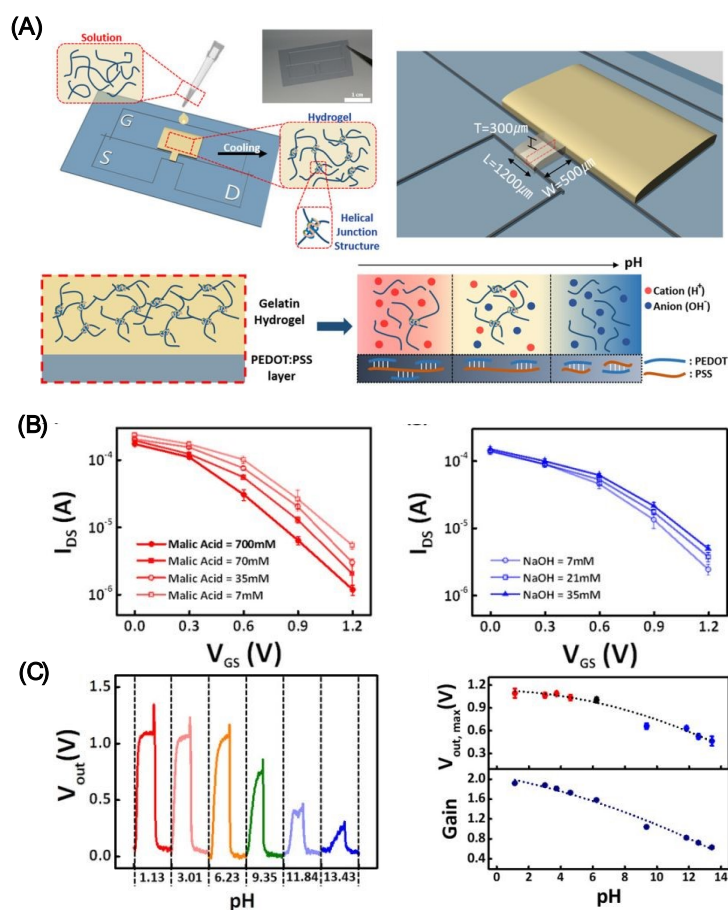


1 solvents⁸³), biological signals (e.g., enzymes⁹⁰, antigens⁹¹) and physical factors (e.g.,
2 light⁹², temperature⁹³, magnetic fields⁹⁴, electric fields⁹⁵, and ultrasound⁹⁶).
3 Consequently, hydrogels find extensive utility across diverse fields, spanning drug
4 delivery⁹⁷, biosensors⁸³, biomimetic materials⁸⁷, and regenerative medicine⁹⁸.

5 Tae-il Kim³⁷ pioneered the development of pH-responsive solid OECTs utilizing
6 gelatin hydrogels. In this design, the transistor channel (PEDOT:PSS) and electrodes
7 were fabricated on a flexible polyethylene terephthalate (PET) substrate. Gelatin served
8 as a solid electrolyte medium, facilitating ion migration from the gate into the channel.
9 The gelatin material was modified with acids and bases additives to introduce mobile
10 cations and anions, enabling their facile penetration into the PEDOT:PSS interface
11 (**Figure 3A**). Interaction with acidic and alkaline gelatin led to alterations in the
12 chemical structure and conductivity of PEDOT:PSS channels. Specifically, acidic
13 hydrogels enhanced the conductivity of PEDOT:PSS, leading to elevated output
14 voltage (V_{out}) and gain, whereas alkaline hydrogels decreased conductivity, resulting in
15 decreased V_{out} and gain (**Figure 3B**). Integration of PEDOT:PSS with gelatin hydrogels
16 of varying pH conditions allowed for modulation of OECTs resistance, V_{out} , and gain.
17 Notably, the maximum output voltage and gain of the inverter were governed by the
18 pH conditions of the hydrogel, ranging from 1.1 to 0.46 V and 1.92 to 0.63 at pH =
19 1.13-13.43, respectively (**Figure 3C**).

View Article Online
DOI: 10.1039/D4TA05288A





1
2 **Figure 3.** (A) Gelatin based-OECTs and its sensitivity to pH. The manipulation of
3 mobile ion concentration and polymeric chain in the gelatin-OECT is achieved through
4 the introduction of acidic and basic substances to the original gelatin composition. (B)
5 Transfer curves of gelatin based-OECTs with changing pH. (C) The pH-dependent
6 characteristics of the maximum output voltage ($V_{out,max}$) and gain of the inverters with
7 the gelatin based-OECTs. Reproduced with permission³⁷. Copyright 2018, American
8 Chemical Society.

9 2.2.4 Temperature-resistance

10 The application of hydrogel electrolytes in solid-state OECTs is hindered by
11 temperature variations, as the inherent structure of hydrogel materials, predominantly
12 water, renders them susceptible to temperature extremes. High temperatures accelerate
13 water loss from hydrogels, while low temperatures cause freezing, both of which
14 compromise their functionality. Additionally, dry environments can detrimentally



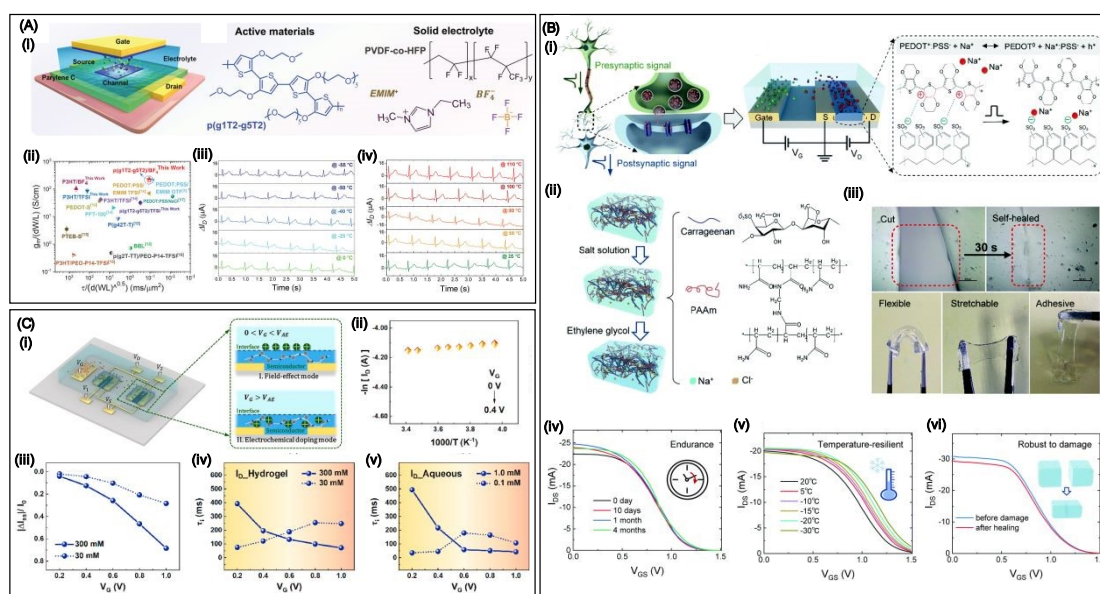
1 affect the durability and conductivity of hydrogels. To enable continuous operation of
2 solid-state OECTs across diverse temperature conditions, efforts have been directed
3 towards enhancing the anti-freeze water-retention properties of hydrogel electrolytes.

4 Studies utilizing IL gels, such as [EMIM][TFSI]⁹⁹, [DEME][TFSI]¹⁰⁰ and
5 [EMI][TFSI]¹⁰¹), have demonstrated improved stability of OECTs. For example,
6 Someya and colleagues⁴⁴ pioneered the utilization of non-volatile dilute IL gel as
7 electrolytes in flexible OECTs, enabling continuous monitoring of electrocardiogram
8 signals for over 3 hours with the device remaining functional for over a week. In 2023,
9 Wei Lin Leong⁷⁸ and colleagues developed IL gel electrolyte consisting of
10 poly(vinylidene fluoride-co-hexafluoropropylene) (PVDF-co-HFP) and IL of 1-ethyl-
11 3-methylimidazolium tetrafluoroborate (EMIM BF₄). The solid-state OECTs,
12 constructed by an active material (thiophene backbone functionalized with glycolated
13 side chains (p(g1T2-g5T2))) and IL gel electrolyte (**Figure 4Ai**), exhibited great
14 performance with high transconductance of $220 \pm 59 \text{ S cm}^{-1}$, ultrafast device speed of
15 10 kHz, and excellent operational stability over 10000 cycles (**Figure 4Aii**). Due to the
16 excellent thermal stability of channel and electrolyte, the devices demonstrated reliable
17 collection of electrophysiological signals even at extreme temperatures (-50 and 110 °C)
18 (**Figure 4Aiii-iv**). Its transient speed was approximately twice as fast as those operating
19 in 0.1 m NaCl electrolyte, benefiting from the low hydration level of the doping anions
20 in the IL gel electrolyte. However, IL gels still exhibit drawbacks including biotoxicity,
21 high cost, and slow ion diffusion¹⁰².

22 Inspired by biological synapses, Qing Wan and colleagues³⁶ devised a hydrogel-based
23 electrochemical transistor (HECT) featuring a transmission-like process (**Figure 4Bi**).
24 A dual-network (DN) hydrogel composed of PAAm and carrageenan was synthesized
25 *via* a one-step free radical polymerization. Sequential immersion in NaCl(a.q.) and
26 ethylene glycol endows it with great electrical performance and long-term stability,
27 facilitating rapid self-repair, anti-freezing, and water-retention properties (**Figure 4Bii**)



1 and **4Biii**). The HECT exhibited excellent biocompatibility and could operate
 2 effectively under harsh conditions for over 4 months or as low as -30°C (**Figure 4Biv-**
 3 **v**). Moreover, the self-healing capability of the hydrogel allowed for the full restoration
 4 of HECT electrical performance, showcasing the device's resilience against accidental
 5 damage. (**Figure 4Bvi**). Similarly, Chuan Liu and colleagues⁵⁸ developed anti-freeze
 6 and water-retaining DN hydrogel electrolytes for solid-state dual-channel OECTs
 7 (**Figure 4Ci**). These hydrogel electrolyte posse good biocompatibility, high ionic
 8 conductivity, and stable operation across a wide temperature range from room
 9 temperature to -30°C (**Figure 4Cii-iii**). Furthermore, the devices can continuously
 10 monitor ion movement during OECT operation through transient currents detection and
 11 in situ multipoint dynamic measurements of central potential (**Figure 4Civ-v**).



12
 13 **Figure 4.** (A) Schematic of solid-state OECTs constructed by active materials of
 14 p(g1T2-g5T2) and IL gel electrolyte (i). (ii) Comparisons of OECTs in this work with
 15 previously reported ones in terms of steady- and transient-state performance. (iii)-(iv)
 16 ECG signals acquired by OECTs at extremely temperatures. Reproduced with
 17 permission⁷⁸. Copyright 2023, Wiley-VCH. (B) The schematic illustration and
 18 characterization of DN hydrogel-based HECT. Schematic illustration of the DN
 19 hydrogel-based HECT (i)-(ii). (iii) Optical microscope images and photos of the



1 damaged and healed DN hydrogel electrolyte. The stability of the electrical properties
2 of DN hydrogel-based HECT including transfer characteristics evaluated over time **(iv)**,
3 at different temperatures **(v)** and damaged and healed states **(vi)**. Reproduced with
4 permission³⁶. Copyright 2021, Royal Society of Chemistry. **(C)** The schematic
5 illustration and characterization of DN hydrogel-based dual-channel OECTs. **(i)**
6 Schematic structure of the DN hydrogel-based dual-channel OECTs. **(ii)- (iii)**
7 Temperature dependence of dual-channel OECTs at various electrolyte concentration.
8 **(iv)-(v)** Drain current behaviour under pulsed gate excitation with hydrogel containing
9 various KCl(a.q.) concentraion. Reproduced with permission⁵⁸. Copyright 2022,
10 Elsevier.

11 **2.2.5 Self-adhesiveness**

12 Self-adhesiveness is a critical property of hydrogels for various applications, including
13 bioelectronic sensors, and tissue engineering and repair. It ensures stable contacts
14 between hydrogel devices and tissues, thereby enhancing overall performance¹⁰³⁻¹⁰⁵.
15 Achieving adhesion involves introducing physical interactions and chemical bonds
16 between hydrogels and substrates, including hydrogen bonding, hydrophobic
17 interactions, metal complexation, π - π stacking, cation- π interactions, and covalent
18 bonding¹⁰⁶⁻¹⁰⁷. Hydrogel electrolytes with high adhesive strength facilitate full contact
19 with the channel, enabling effective ion penetration and transport to the active channel
20 layer³⁵. Besides, many sensing functions of OECTs require direct connection of their
21 semiconductor channels to tissue surfaces, allowing electrostatic modulation of bulk
22 conductivity by biopotential or targeted biochemical signals¹⁰⁸⁻¹⁰⁹. The optimal
23 interface involves direct adhesion of the semiconductor channel to the tissue surface¹¹⁰,
24 as biological signal transduction depends on the microscale distance between the
25 semiconducting channel and the tissue surface¹¹¹. Gels serve as a pliable medium that
26 facilitates the interaction between electronic devices and biological systems,, enhancing
27 contact and adhesion^{2, 44}.



1 Shiming Zhang³⁴ introduced an OECT-based continuous glucose monitoring (OECT-
2 CGM) system comprising a hollow microneedle patch, an adhesive glucose oxidase
3 (GO_x)-loaded DN hydrogel film, and OECT glucose sensors (**Figure 5Ai-ii**). The
4 microneedles provide a minimally invasive interface between interstitial fluid (ISF) and
5 the OECT-CGM system. The adhesive DN hydrogel film, synthesized with an
6 interpenetrating network (IPN) structure of PAAm and sodium alginate loaded with
7 GO_x, serves as the gel electrolyte of the OECTs. This structure not only enhances the
8 stability of the interface between the skin and device during movement but also
9 facilitates the diffusion of glucose molecules from the ISF to the OECT-CGM system
10 *via* the microneedles and hydrogel. This diffusion alters the current in the OECTs,
11 enabling glucose monitoring (**Figure 5Aiii-vi**). Moreover, previous studies has
12 leveraged the adhesive hydrogels for transferring conductive polymer films in OECTs
13 applications. This approach facilitates the transfer of conductive polymer films from
14 rigid to flexible substrates, addressing the difficulty of directly handling conductive
15 polymers on flexible materials¹¹²⁻¹¹³. For instance, Ali Khademhosseini¹¹⁴ employed
16 hydrogel electrolytes to facilitate the transfer of conductive polymer films from
17 traditional rigid substrates to flexible ones (**Figure 5B**). Initially, PEDOT:PSS
18 suspension, combined with surfactants like dodecylbenzenesulfonic acid (DBSA), was
19 patterned on glass substrates. The DBSA reduced the adhesion between the
20 PEDOT:PSS film and the glass substrate. Given the stronger adhesion between
21 PEDOT:PSS and the hydrogel, PEDOT:PSS could be easily transferred to various soft
22 substrates (**Figure 5Bi-vi**). This technique enabled the creation of OECTs that are
23 conformable and attachable to the skin, demonstrating high transconductance and a
24 significant on/off ratio (**Figure 5Bvii-x**). These OECTs maintained stable performance
25 even when subjected to mechanical deformation of the skin. By integrating OECTs with
26 mobile electronic devices, a portable electronic readout system for glucose
27 concentration monitoring was developed.



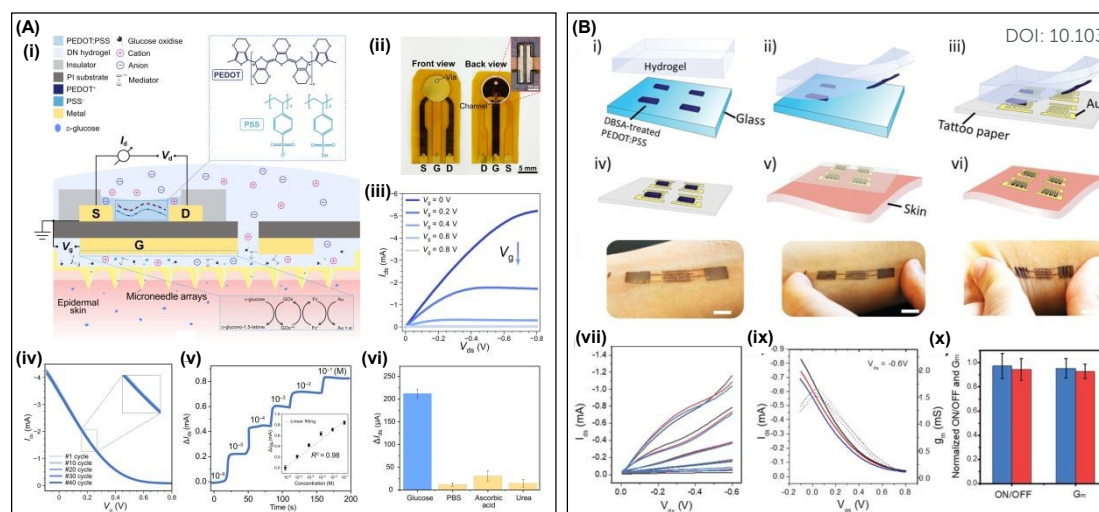


Figure 5. (A) Fabrication and characterization of OECT-CGM. Schematic (i) and photos (ii) of the OECT-CGM and the sensing mechanism. Output curves (iii) and Transfer curves (iv) of flexible OECTs. (v)-(vi) Response of OECT-CGM. Reproduced with permission³⁴. Copyright 2024, AAAS. (B) Transferring process of PEDOT:PSS films and its soft OECTs performance. (i)-(vi) Schematic illustration of the generic process for transferring PEDOT:PSS films with the help of hydrogel electrolyte. (vii)-(ix) Output and transfer curves of OECTs at released (red), 5% stretched (blue) and 40% compressed (black) conditions; (x) on/off ratio and transconductance of initial OECTs and after compressed for 10 times. Reproduced with permission¹¹⁴. Copyright 2020, Wiley-VCH.

2.2.6 Stretchability

Stretchable electronic devices have garnered great attention in bioelectronics because they maintain functionality when subjected to mechanical deformation. This property is particularly valuable for applications requiring close contact with curved surfaces or sensitivity to movement, such as artificial skin, implantable electronic devices, and wearable health monitors¹¹⁵⁻¹¹⁶. Wearable electronic devices must conform to the skin and endure bending, twisting, and stretching¹¹⁷. Several studies have demonstrated that gel-based OECTs have been identified as promising candidates for stretchable bioelectronics¹¹⁸⁻¹¹⁹. The high sensitivity of stretchable OECTs in wearable and

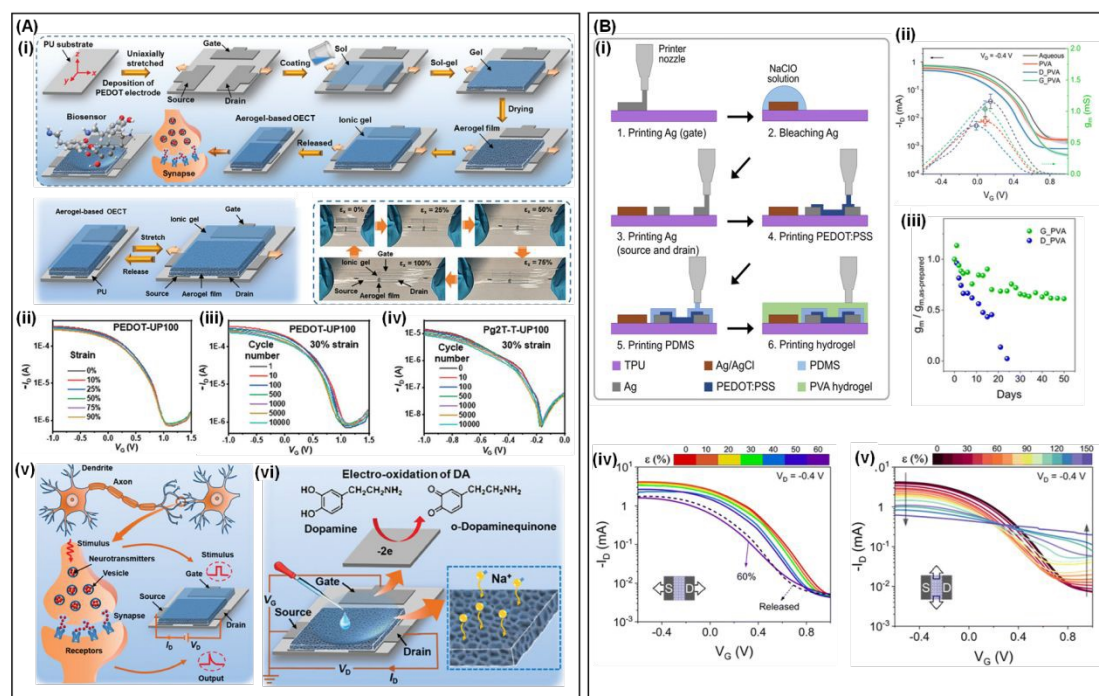


1 implantable biosensing and bioelectronic is crucial due to their skin-like softness and
2 stretchability, which enable seamless integration with curved skin or tissue surfaces¹²⁰.
3 The stretchable solid-state OECTs enhances biocompatibility, daily usage comfort, and
4 high-fidelity signal transduction¹²¹.

5 Sihong Wang¹¹⁹ and colleagues successfully fabricated OECTs with high
6 transconductance (223 S cm^{-1}), biaxial stretchability (100% of strain) and excellent
7 skin compliance. This was achieved using a polymerized stretchable semiconducting
8 polymer, poly(2-(3,3'-bis(2-(2-(2-methoxyethoxy)ethoxy)ethoxy)-[2,2'-bithiophen]-5-
9 yl)thiophene) (p(g2T-T)), and commercially available gel electrolytes. Guoqing Zu¹²²
10 prepared stretchable OECTs using stretchable active material and gel electrolyte.
11 PEDOT-based aerogel films or poly(2,5-bis(3-triethyleneglycoloxythiophen-2-yl)-co-
12 thiophene) (Pg2T-T)-based aerogel films, prepared *via* spin coating, sol-gel and freeze-
13 drying protocols, served as the active layer. The polymer sol is spin-coated on a pre-
14 stretched polyurethane (PU) to create stretchable semiconducting polymer-based
15 aerogel films. Stretchable PAAm ion gel or ionic liquid (tris(2-hydroxyethyl)methyl
16 ammonium methyl sulfate) was used as electrolyte (**Figure 6Ai**). This OECT exhibits
17 a high on/off ratio, high transconductance, stretchability up to 100%, and tensile
18 stability for 10,000 cycles at 30% strain (**Figure 6Aii-iv**). It can also serve as a
19 stretchable artificial synapse and biosensor for detecting dopamine (DA) (**Figure 6Av-
20 vi**). Fabio Cicoira³⁸ utilized a printed circuit board printer to fabricate fully printed and
21 stretchable OECTs on stretchable PU (**Figure 6Bi**). To ensure overall device
22 stretchability, printed planar gate electrodes and polyvinyl alcohol (PVA) hydrogel
23 electrolytes were used. Flexible functionality was achieved using Ag paste for the drain,
24 source, and gate electrodes. The PVA precursor ink was printed on the channel and gate
25 electrodes, and crosslinked through freeze-thawing process, i.e., storing at -15°C for 12
26 hours followed by thawing at room temperature. The transconductance ($1.04 \pm 0.13 \text{ mS}$)
27 and on/off ratio (830) of resulting OECTs are comparable to inkjet or screen-printed



1 OECTs (**Figure 6Bii**). It can maintain operation for at least 50 days, with the
 2 transconductance remaining 60% of its initial value (**Figure 6Biii**). Notably, the device
 3 exhibited stretchability of 60% along the channel direction and 150% in the
 4 perpendicular direction (**Figure 6Biv-v**), making it well-suited for the mechanical
 5 deformations encountered in wearable electronic products.



6 **Figure 6.** (A) Fabrication and applications of semiconducting aerogel film-based
 7 OECTs. (i) The schematic illustration of semiconducting aerogel film and stretchable
 8 OECTs. The schematic illustration of fabricating the printed OECTs. (ii)-(iv) Transfer
 9 curves of OECTs based on with various tensile strains and during stretching-releasing
 10 process for 10000 cycles. (v)-(vi) The artificial synapse and biosensor of the
 11 semiconducting aerogel film-based OECTs. Reproduced with permission¹²². Copyright
 12 2024, Wiley-VCH. (B) Preparation and characterization of printed and stretchable
 13 OECTs using PVA hydrogel electrolytes. (i) Step diagram of fabricating the printed
 14 OECTs. (ii) Transfer and transconductance curves of electrolytes. (iii) Long-term
 15 stability tests of OECTs. Transfer curves under strain in a length direction (iv) and
 16 width direction (v) of the active channel. Reproduced with permission³⁸. Copyright



1 2023, Royal Society of Chemistry.

2 Gel electrolytes applied in OECTs offer those advantages discussed above, yet they
3 face various challenges and drawbacks. Self-healing capability may be constrained by
4 environmental conditions, limiting the complete restoration of mechanical and
5 electrical properties in practical applications. High stretchability can relax the material,
6 reducing stability and electrical conductivity. Mechanical stress during stretching may
7 cause delamination or failure at interfaces with other materials. Responsive hydrogel
8 electrolytes may make OECTs highly sensitive to external stimuli, potentially causing
9 false detections or erroneous responses under non-ideal conditions like noise or
10 environmental variations; prolonged repetitive stimuli could induce material fatigue,
11 affecting response speed and accuracy. To maintain thermal stability, hydrogel
12 electrolytes require compatible electrodes to prevent changes in physicochemical
13 properties at high temperatures, potentially reducing device lifespan. Moreover, the
14 adhesive properties of gels are sensitive to environmental changes such as temperature
15 and humidity, potentially affecting the reliability and accuracy of OECTs sensing
16 capabilities.

17 **3. Application**

18 OECTs utilizing hydrogel electrolytes provide an ideal interface with biological
19 environments due to their inherent biocompatibility and mechanical compatibility.
20 These devices offer local signal amplification, resulting in high-fidelity sensor
21 detection, which is crucial for bioelectronics applications. A common strategy involves
22 modifying the gate electrode to control its electrochemical potential, thereby converting
23 various biological signals¹²³⁻¹²⁴. Rapid cyclic voltammetry serves as a convenient
24 characterization method for OECTs, offering speed and cost-effectiveness compared to
25 alternative techniques.

26 The use of OECTs for detecting target biomarkers amidst interfering elements provides



1 several advantages, including high selectivity, sensitivity, and low detection limits.¹²⁵
2 Preliminary research has highlighted the significant potential of OECTs in detecting
3 various ions¹²⁶⁻¹²⁸, biomolecules (such as enzyme¹²⁹, cortisol¹³⁰, immune¹³¹, glucose¹³²⁻
4 ¹³³, and metabolite¹³⁴ detection), as well as physiological signals (such as EMG¹³⁵⁻¹³⁶
5 and ECG¹³⁷). This section will delve into the exploration of solid-state OECTs based
6 on gel electrolytes in biosensing and bioelectronics applications.

7 **3.1 Biosensor**

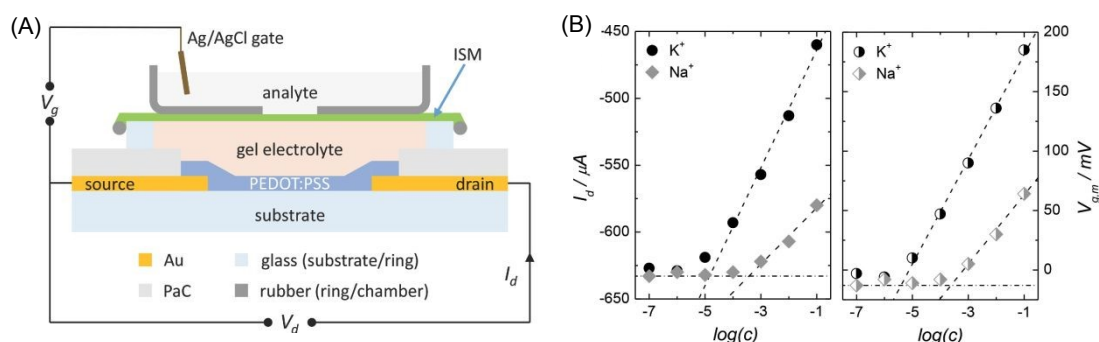
8 **3.1.1 Ion sensor**

9 Ion sensing is crucial for various applications, such as sports performance tracking,
10 health monitoring, and clinical diagnostics. Research in ion sensing has primarily
11 focused on three ions: K⁺, Na⁺, and Ca²⁺. K⁺ and Na⁺ are essential for
12 transmitting nerve impulses, muscle contraction and relaxation, and maintaining proper
13 water balance across cell membranes¹³⁸. Ca²⁺ is essential for building and maintaining
14 strong bones, teeth, and nails¹³⁹. Abnormal levels of these cation can indicate various
15 functional disorders, including dehydration, uncontrolled diabetes, and kidney
16 failure¹⁴⁰. Changes in ion concentrations in electrolytes typically influence electrical
17 signal of the OECTs¹⁴¹, making them valuable tools for ion sensing in healthcare and
18 disease diagnosis.

19 Ionic sensitive and selective OECTs have been successfully developed for various ion
20 sensor, with notable progress in selective ion sensing applications using solid-state
21 OECTs with hydrogel electrolytes. For instance, in 2014, Michele Sessolo³⁹ developed
22 a fully solid-state OECT for K⁺ selectivity utilizing a hydrogel electrolyte. The device
23 integrates a polymer membrane allowing specific ions to pass (K⁺-selective electrodes
24 (ISM)) with the OECTs, employing a hydrogel as the electrolyte in contact with the
25 PEDOT:PSS channel. **Figure 7A** illustrates the layout of the ion-selective OECTs. The
26 ISM is placed between the hydrogel electrolyte and the target electrolyte, isolating the



1 channel from the gate of the OECTs. The hydrogel electrolyte, prepared by gelation at
 2 room temperature from a dispersion containing agarose, KCl, and
 3 ethylenediaminetetraacetic acid disodium salt (Na₂EDTA) as a thermal precursor,
 4 maintain K⁺ selectivity¹⁴². The decrease in drain current proportional to K⁺
 5 concentration was observed, attributed to an increase in the number of permeating K⁺
 6 ions or a reduction in electrolyte resistance. Sensitivity to K⁺ was much higher than to
 7 Na⁺, confirming the membrane's ion selectivity (**Figure 7B**). Additionally, the authors
 8 successfully prepared OECTs for asynchronous ion-selective sensing of other cation
 9 (K⁺, Ca²⁺, and Ag⁺)¹⁴³ as well as synchronous ion-selective sensing of Ca²⁺ and NH₄⁺
 10 in sweat using different ISMs¹⁴⁴. Replacing the ion solution electrolyte with a hydrogel
 11 electrolyte represents an effective approach for fabricating solid-state OECTs for
 12 multifunctional ion-selective specific sensing in the future.



13

14 **Figure 7.** (A) Schematic of K⁺-selective OECTs. (B) Calibration curves of different
 15 ionic solutions performed using K⁺-selective OECTs. Reproduced with permission³⁹.
 16 Copyright 2014, Wiley-VCH.

17 3.1.2 Metabolite detection

18 OECTs also function as metabolite sensors, playing a critical role in clinical diagnostics
 19 and health monitoring. They detect intermediate or final products of metabolism, and
 20 changes in metabolic rates can indicate the presence of disease¹⁴⁵. Metabolite sensing
 21 with OECTs can be categorized into two types: electroactive metabolites undergoing



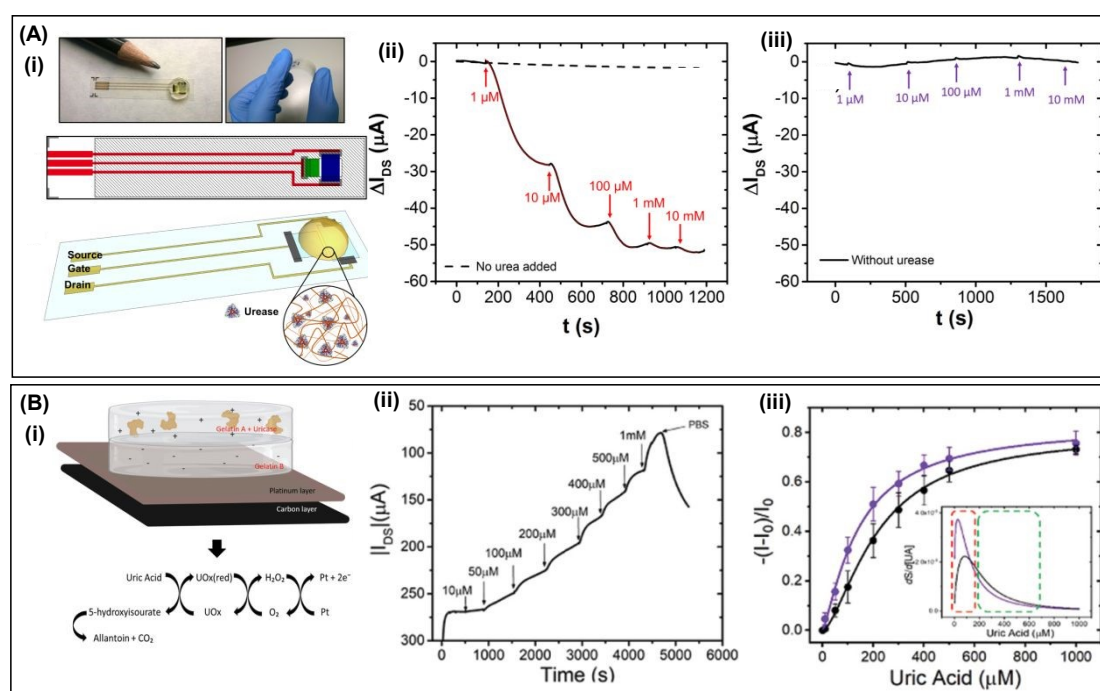
1 oxidation-reduction reactions on the electrode, and specific reactions of
2 oxidoreductases with metabolite molecules. Examples of the first type include
3 dopamine (DA)¹⁴⁶, ascorbic acid¹⁴⁷, and uric acid (UA)¹⁴⁸⁻¹⁴⁹. Conversely, metabolites
4 that undergo specific reactions with oxidoreductases include glucose^{57, 150-151}, lactate¹⁵²⁻
5 ¹⁵³, cortisol¹⁵⁴, as well as nucleic acids and amino acids¹⁵⁵. Both types rely on changes
6 in channel current corresponding to metabolite concentration in the electrolyte.

7 In recent years, solid-state OECTs based on hydrogel electrolytes have made significant
8 progress in detecting metabolites. Researchers have achieved specific detection of
9 metabolites through clever design of hydrogel functional groups or structures. For
10 instance, Carlo A Bortolott et al.⁴⁰ developed a flexible urea OECT-based biosensor by
11 depositing cross-linked gelatin hydrogel doped with urease onto fully printed
12 PEDOT:PSS channel material (**Figure 8Ai**). The ion substances produced by urease-
13 catalyzed urea hydrolysis regulate the channel conductivity, enabling urea detection.
14 Gelatin/Tris hydrogel ensured the retention of protein catalytic activity and enabled
15 selective penetration of NH₄⁺ to the PEDOT:PSS channel for response specificity. This
16 biosensor exhibited a response time of 2-3 minutes, a limit of detection of 1 μM, and a
17 dynamic range spanning three orders of magnitude, making it suitable for urea detection
18 in biological samples (**Figure 8Aii-iii**). Given urea's significance in clinical analysis,
19 especially in chronic kidney disease (CKD) monitoring, the low operating voltage (<0.5
20 V) of this biosensor makes it an attractive candidate for high-throughput CKD
21 monitoring at care points or on-site¹⁵⁶.

22 Similarly, in another study, a low-cost, disposable OECT sensor for detecting UA was
23 developed⁴¹. The sensor utilized a double-layer hydrogel composed of polycations and
24 polyanions gelatin with opposite charges as the electrolyte. UA detection relied on the
25 catalytic activity of uricase (UO_x), ultimately generating H₂O₂ (**Figure 8Bi**). The
26 double-layer hydrogel electrolyte acted as a charge-selective barrier, permitting H₂O₂
27 diffusion to the gate electrode for oxidation while suppressing Faradaic reactions from



1 the oxidation of electroactive molecules. Specifically, Gelatin A layer consisted of a
 2 polymer network with positive charges and mobile anions to balance its charge,
 3 enhancing selectivity by hindering cation diffusion to the gate electrode. It crosslinked
 4 with UO_x , penetrating UA to react with uricase inside the gel network, catalyzing it into
 5 5-hydroxyisourate, and ultimately converting it to allantoin spontaneously. Gelatin B,
 6 composed of a negatively charged network with mobile counterbalancing cations,
 7 prevented the diffusion of anionic electroactive substances to the gate electrode, thereby
 8 enabling potential Faradaic response. This OECT-based biosensor could operate in
 9 artificial biological fluids while maintaining sensitivity similar to that in model
 10 solutions such as PBS buffer and artificial wound exudate (**Figure 8Bii-iii**). Elevated
 11 UA levels occur due to malnutrition¹⁵⁷, metabolic disorders, or diseases such as cancer
 12 or diabetes¹⁵⁸, resulting in phenomena such as urate crystal deposition in joints and
 13 kidneys and gout¹⁵⁹. These examples illustrate the potential of solid-state OECTs with
 14 hydrogel electrolytes in metabolite sensing, offering promising avenues for clinical
 15 diagnostics and health monitoring.



16

17 **Figure 8.** (A) (i) Photographs and schematic of the a flexible OECT-based biosensor

1 for urea detection. **(ii)-(iii)** The current changes of OECT-based urea sensor response
2 to different concentrations of urea for hydrogel prepared by crosslinked urease in
3 gelatin and controlled hydrogel without crosslinked urease. Reproduced with
4 permission⁴⁰. Copyright 2018, IOP publishing, Ltd. **(B) (i)** Schematic structure of
5 OECT biosensor and the mechanism of UA detection. (ii)-(iii) shows the UA detection
6 performance. **(ii)** Real-time drain current changes as a function of UA concentrations.
7 **(iii)** Normalized current change at changing UA concentrations in PBS (black dots) and
8 artificial wound exudate (violet dots). Reproduced with permission⁴¹. Copyright 2020,
9 Wiley-VCH.

10 Toshiya Sakata and colleagues⁴² developed an OECT for glucose sensing utilizing a
11 DN hydrogel. The authors synthesized the DN conductive hydrogel by polymerizing
12 acrylamide (AAm) in PEDOT:PSS dispersion. The first network comprised of
13 PEDOT:PSS, while the second network was composed of PAAm incorporating
14 sulfonic acid to improve compatibility with PEDOT and phenylboronic acid (PBA) to
15 enhance glucose-specific affinity (**Figure 9A**). This hydrogel exhibited excellent
16 conductivity (20 S cm^{-1} in PBS) and hydration properties similar to soft biological
17 tissues. By employing a simple thermal-mechanical annealing process, low-resistance
18 contacts with gold electrodes were established. Remarkably, the hydrogel remained
19 stable even after continuous immersion for one month, effectively serving as the
20 channel for OECTs. The equilibrium boronate esterification on PBA, coupled with
21 catalytic O_2 reduction on PEDOT, enabled the direct detection and amplification of
22 electrochemical signals originating from glucose concentrations (**Figure 9B-D**). The
23 OECTs demonstrated a transconductance of 40 mS and an on/off ratio of 10^3 , allowing
24 for linear mode operation with exceptional conductivity.



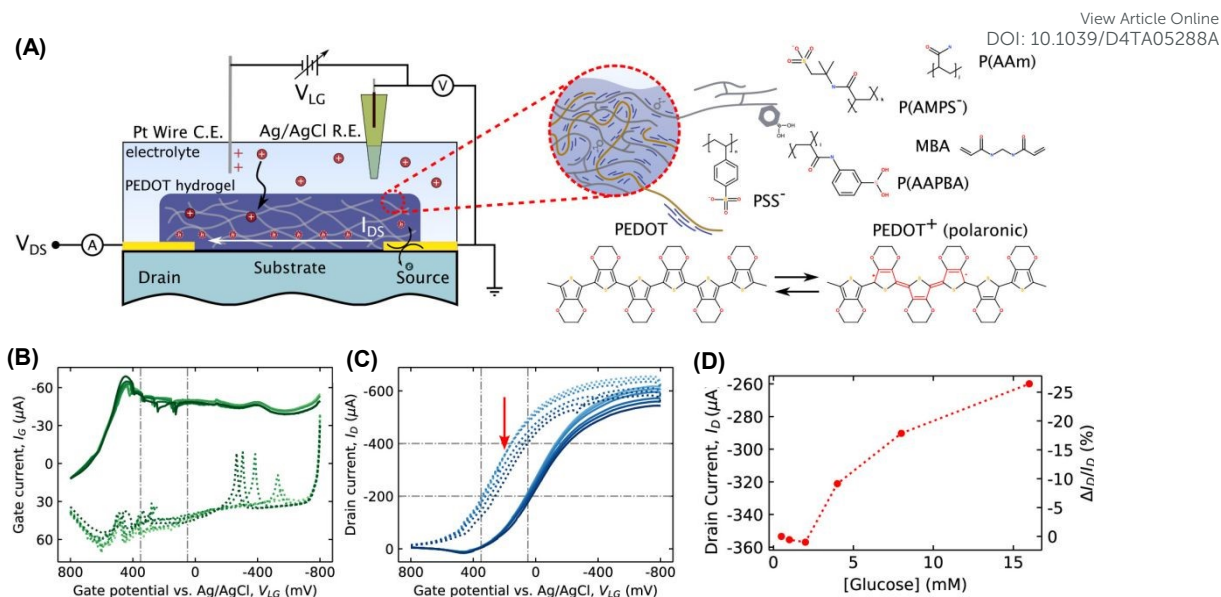


Figure 9. (A) Schematic and mechanism of DN hydrogel-based OECTs for glucose sensing. The concurrent gate leakage (B) and transfer curves (C) during glucose sensing (Darker shades and Dot-dashed correspond to high and low glucose concentration, respectively). (D) extracted from the midpoint potential of the ROI as indicated by the red arrow in (C). Reproduced with permission⁴². Copyright 2022, American Chemical Society.

3.2 Electrophysiological signals detection

Investigating neural tissues and activities through recording and stimulation offers valuable insights into the physiological and pathological functions of the body and brain. While electrocardiography remains pivotal for capturing cardiac activity, traditional metal electrodes are not ideal for brain connectivity due to their rigidity, which leads to tissue damage and inflammation. Moreover, these electrodes are prone to noise interference from transmission lines and external circuits, reducing their effectiveness. Achieving high-quality electroencephalogram (EEG) and electrocardiography (ECG) signals often requires strong chemical adhesives to bond electrodes to the scalp surface or intracranially, potentially causing tissue damage and immune system reactions in the brain^{13, 160}. Soft and flexible materials utilized in OECTs offer a promising solution by



1 directly amplify input signals recorded from the site, making them ideal for measuring
2 electrophysiological signals. To ensure stable and long-term measurements, hydrogels
3 or IL gels are used to improve interaction between electronic devices and the skin,
4 thereby providing valuable techniques for study and diagnosis brain-related diseases.

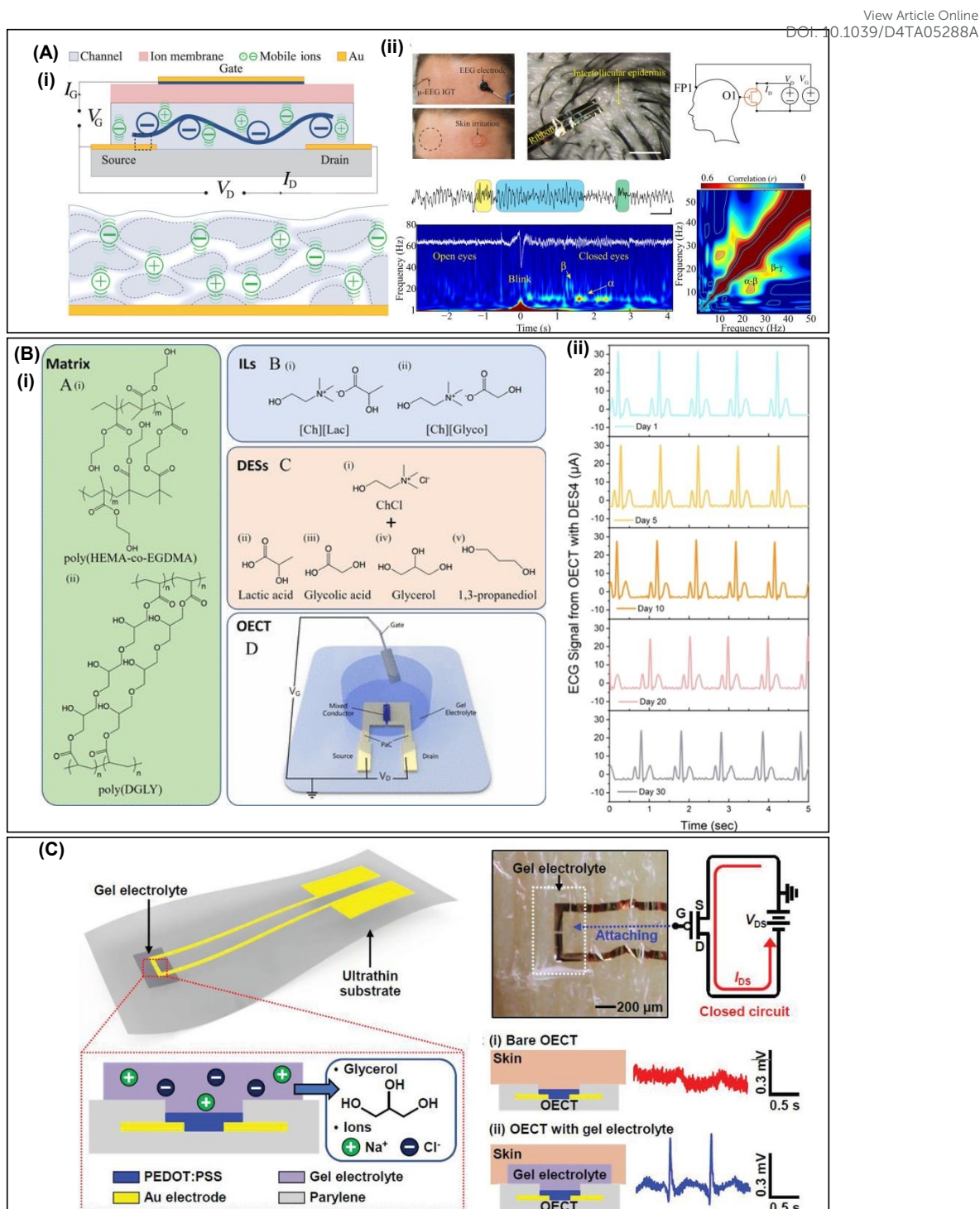
5 Khodagholy and colleagues⁴³ devised a flexible, biocompatible, internal ion-gated
6 OECTs that features high transconductance, rapid response time, and great
7 conformability to amplify and record high-quality neural physiological activities (EEG)
8 in the brain (**Figure 10Ai**). This device uses a conductive polymer PEDOT:PSS,
9 combined with D-sorbitol to form an ionic reservoir, which facilitates ion transport
10 channels and enhances the conductivity of PEDOT:PSS. Chitosan hydrogel serves as
11 an ion membrane between the gate and channel, offering biocompatibility, stability,
12 and solution processability. This minimizes electrochemical impedance at the interface
13 skin-electrode interface, thus reducing skin redness or irritation. This OECTs
14 successfully captured clear neural oscillations at approximately 8-12 Hz (α) from the
15 occipital area during wakeful closed eyes, consistent with posterior-dominant rhythm
16 (**Figure 10Aii**). It also recorded higher-frequency brain oscillations occurring
17 simultaneously at (13-25 Hz, β) and (30-50 Hz, γ), highlighting the OECT's capability
18 to perform various neural computations and information transmission between cortical
19 areas.

20 Sahika Inal et al.⁵³ developed three types of gel electrolytes with the same polymer
21 matrices but different ionic components: saline solutions, ILs, and Deep eutectic
22 solvents (DESs). These electrolytes were evaluated for their performance in OECTs to
23 study the influence of electrolyte types on OECT properties (**Figure 10Bi**). The DES
24 electrolyte, prepared with poly (diglycidyl ether of bisphenol-A) (DGLY) as the
25 polymer matrix and choline chloride (ChCl) with 1,3-propanediol as the ionic
26 components, outperformed the other two gel electrolytes, in p-type depletion-mode and
27 p-type and n-type enhancement-mode OECTs. This OECTs demonstrated excellent



1 stability in long-term ECG signal monitoring, maintaining a consistent signal-to-noise
2 ratio (SNR) even after 5 hours and 30 days of continuous operation (**Figure 10Bii**).
3 Takao Someya et al.⁴⁴ reported ultra-thin wearable OECTs for detecting ECG based on
4 non-volatile hydrogel electrolytes, capable of operating on dry biological surfaces. The
5 gel electrolyte consists of a dispersed phase of glycerol-ionic solution and a matrix of
6 PVA and PAAm (**Figure 10Ci**). The low volatility of glycerol ensure stability, anti-
7 drying properties. The gel also maintains good mechanical stability under physical
8 deformation. Moreover, the developed OECTs can uniformly adhere to the skin,
9 effectively monitoring cardiac signals from the skin continuously for long-term
10 applications (**Figure 10Cii**), thus overcoming the contact limitations of previous
11 OECTs.





1
2 **Figure 10.** (A) (i) Schematic illustration of OECTs and (ii) Recording of EEG signals
3 recording by OECTs that attached on human scalp during opening and closing eyes.
4 Reproduced with permission⁴³. Copyright 2019, AAAS. (B) (i) Chemical structures of
5 the gel electrolyte and the OECTs architecture. (ii) ECG acquisition with a best
6 eutectogel-gated OECTs. Reproduced with permission⁵³. CC BY 4.0. (C) Architecture



1 of ultrathin wearable OECT with nonvolatile gel electrolyte and its application on ECG
 2 measurement from the skin. Reproduced with permission⁴⁴. Copyright 2019, Wiley-
 3 VCH.

4 The current existing solid-state OECT based on gel electrolyte and their performance
 5 are concluded and compared in **Table 1**. The development of solid-state OECT has
 6 progressed from incorporating soft gel electrolytes with various properties to creating
 7 high-performance OECT, and finally to integrating these devices into wearable or
 8 implantable biosensors and bioelectronics.

9 **Table 1.** Comparison of current solid-state OECT based on gel electrolyte.

Gel electrolyte	Gelation method	Properties and functions	Main parameters	Application	Ref.
PVA	freezing-thawing	Self-healing	Self-healing ratio:85%-100%	ion sensor (detect Na ⁺)	35
Gelatin	Heating-cooling	pH-responsive	Vout and gain range from 1.1 to 0.46 V and 1.92 to 0.63 at pH = 1.13-13.43	electrochemical logic circuits (NOT, NOR, and NAND gates)	37
PVA-PAAm	Photolithography and photo polymerization	Flexible, Nonvolatile	> 8 days stability	ECG monitoring	44
IL gel composite of PVDF-co-HFP and EMIM BF4	spin-coating	Wide temperature-resistance	Transient speed values are ≈0.1 ms at 25 °C and ≈1.9 ms at -40 °C.	ECG monitoring	78
DN hydrogel (PAAm/ carrageenan)	Thermal polymerization	Temperature-resistance	> 4 months stability; operation at -30 °C ~20°C.	mimic synaptic functions	36
DN hydrogel (PAAm/ carrageenan)	Thermal polymerization	Temperature-resistance	operation at -30 °C ~20°C	ion sensor (detect various [KCl])	58
DN hydrogel (PAAm/ Na+-alginate/ GOx)	Photo polymerization	Adhesion	Great SNR:~60 dB	glucose monitoring	34
PVA/ gelatin; PVA/ agarose	Heating-cooling	Adhesion	Enable transfer-printing of PEDOT:PSS films; Transconductance: ~1.5	glucose monitoring	114



			mS; ON/OFF:~50	View Article Online DOI: 10.1039/D4TA05288A	
Commercial gel (Bio-Protech, T716-50)	-	Stretchability	Transconductance:~223 S cm ⁻¹ ; biaxial stretchability: 100% strain	ECG monitoring	119
PAAm ion gel or ionic liquid (tris(2-hydroxyethyl)methyl ammonium methyl sulfate)	Photo polymerization	Stretchability	high on/off ratio; stretchability:100% strain; tensile stability: 10,000 cycles at 30% strain	DA detecting	122
PVA; Glycerol-PVA; DMSO-PVA	freeze-thawing	Stretchability	transconductance:1.04 ± 0.13 mS; on/off ratio: 830; stretchability: channel direction of ~60% strain and perpendicular direction of 150% strain.	-	38
Agarose/Na2EDTA/ KCl	Heating-cooling	K ⁺ selectivity	High selectivity coefficient (-log K _{K⁺,Na⁺} : 2.7)	ion sensor (detect K ⁺)	39
Gelatin/Tris	Cooling	ensure the retention of protein catalytic activity and enable selective penetration of NH ₄ ⁺	low LODs :1 μM; response time: 2-3 mins	Urea detecting	40
Double-layer opposite- charged hydrogel (polycations and polyanions gelatin)	Crosslinked by glutaraldehyde	Function as a charge-selective barrier	low LODs [UA]: 4.5 × 10 ⁻⁶ M	UA detection	41
DN hydrogel (PEDOT:PSS/PAA m-P AMPS- PBA)	Thermal polymerization	Glucose specific	transconductance: 40 mS; on/off ratio: 10 ³	Glucose Detection	42
Chitosan	Spin-coating	Acting as an ion membrane	Transconductance:32.3 0 mS; >100 days stability	EEG monitoring	43
poly(HEMA-co-	Photo polymerization	Constructing	Transconductance:~27	ECG monitoring	53



EGDMA) and poly(DGLY) with three different ionic components (saline solutions, ILs, and Deep eutectic solvents (DESs))		of p-type depletion and p-type and n-type enhancement mode devices.	mS; ON/OFF ratio: 4.0×10^5 ; switching speed: 24 ms	View Article Online DOI: 10.1039/D4TA05288A	
PVA/PAAm with glycerol-ionic solution	Photolithography and photo polymerization	Anti-drying, long term stability	Transconductance: 1.62 mS; > 8 days stability	ECG monitoring	44
P(VDF-HFP) with [EMI][TFSI]	Drop-casting	Realizing fully printed OECT	Transconductance :1.1 mS	-	161

1 4. Challenges and Perspectives

2 In this comprehensive review, we systematically present the latest advancements in
3 solid-state OECT based on gel electrolyte, encompassing the classification and
4 properties of gel electrolytes. The prolific research conducted on the OECT underscores
5 the persisting demand for their widespread applications. As elucidated, OECT
6 employing gel electrolyte hold promise in various fields such as ion sensors, biosensors,
7 and electrophysiological monitoring devices. Despite significant efforts directed
8 towards exploring novel bioelectronic applications leveraging gel electrolytes for solid-
9 state OECT, several challenges remain to be addressed and improved upon.

10 In terms of manufacturing techniques, traditional OECTs device fabrication involves
11 simple processes like inkjet printing¹⁶² and screen printing²⁸, offering unique
12 advantages for producing low-cost and large-area electronic devices. However, the
13 current approach of manually applying hydrogel electrolytes to OECTs devices
14 constrains their scalability. Although previous work has combined water-based inkjet-
15 printed PEDOT:PSS electrodes and solution-processable ionic gel dielectrics to achieve
16 fully printed OECTs in environmentally friendly solvents¹⁶¹, more work should be
17 systematically exploring and designing hydrogel precursor solutions with tailored
18 viscosities suitable for various printing processes (e.g., low viscosity for inkjet printers



1 and high viscosity for screen printers), studying relevant standard parameters, thereby
2 facilitating their integration into solid-state OECTs through printing processes.

3 Smart solid-state OECT incorporating responsive hydrogel electrolytes are still at
4 nascent stages. Although some examples exist of using acid- and alkali-modified
5 gelatin to prepare electrolytes capable of regulating channel conductivity by modulating
6 the concentration of H^+ and OH^- at the electrolyte-channel interface³⁷, the development
7 of responsive OECTs remains relatively limited. Future endeavors could harness the
8 multi-responsiveness of hydrogel electrolytes (e.g., to ions, temperature, light, electric
9 field, magnetic field, etc.) to design more intelligent solid-state OECTs sensors or
10 bioelectronic devices, thereby broadening their application scenarios. Particularly,
11 integrating drug-controllable loading and release mechanisms into responsive gels
12 could confer dual-functionality for diagnosing and treating diseases using solid-state
13 OECTs. Moreover, by judiciously incorporating various endogenous (chemical and
14 biological) and exogenous (physical) stimuli-responsive units into hydrogel systems, a
15 versatile "toolbox" can be devised to tailor smart OECTs, representing an effective
16 approach to programming or integrating diverse functional OECTs. Additionally,
17 employing biodegradable hydrogel can propel the development of implantable devices
18 for recording or stimulating electrogenic cells.

19 The pursuit of high-density and implantable biochips for real-time health monitoring
20 necessitates self-powered operation, wireless communication, and low-power
21 functionalities. To fulfill these requirements, energy storage devices based on hydrogel
22 electrolytes have been extensively researched¹⁶³⁻¹⁶⁴, including freeze-resistant batteries
23 capable of operating safely at low temperatures¹⁶⁵, stretchable flexible capacitors¹⁶⁶ and
24 batteries¹⁶⁷⁻¹⁶⁸, and long-lasting batteries¹⁶⁹. Integrating solid-state OECTs based on
25 hydrogel electrolytes with hydrogel batteries holds promise for fully flexible, self-
26 powered, and biocompatible solid-state sensors. Moreover, the realization of wireless
27 signal transmission and noise suppression functionalities is anticipated through the



1 integration of OECTs technology and the continuous advancement of current digital
2 circuits.

3 **Declaration of Competing Interest**

4 There are no conflicts to declare.

5 **Acknowledgements**

6 This work was supported by the Shenzhen Fundamental Research Funding
7 (JCYJ20220530113802006), Guangdong Basic and Applied Basic Research
8 Foundation (2023A1515110012), National Natural Science Foundation of China
9 (22405030, 22305047), Dongguan Science and Technology of Social Development
10 Program (20231800939852), as well as the Guangdong Basic and Applied Basic
11 Research Foundation (2023A1515140114), the open research fund of Songshan Lake
12 Materials Laboratory (2022SLABFN06).



1 **References**

- 2 1. Rivnay, J.; Inal, S.; Salleo, A.; Owens, R. M.; Berggren, M.; Malliaras, G. G.,
3 Organic electrochemical transistors. *Nat. Rev. Mater.* **2018**, *3* (2), 1-14.
- 4 2. Someya, T.; Bao, Z.; Malliaras, G. G., The rise of plastic bioelectronics. *Nature*
5 **2016**, *540* (7633), 379-385.
- 6 3. Niu, Y.; Qin, Z.; Zhang, Y.; Chen, C.; Liu, S.; Chen, H., Expanding the potential
7 of biosensors: a review on organic field effect transistor (OFET) and organic
8 electrochemical transistor (OECT) biosensors. *Materials Futures* **2023**, *2* (4), 042401.
- 9 4. Huang, W.; Chen, J.; Yao, Y.; Zheng, D.; Ji, X.; Feng, L.-W.; Moore, D.; Glavin,
10 N. R.; Xie, M.; Chen, Y., Vertical organic electrochemical transistors for
11 complementary circuits. *Nature* **2023**, *613* (7944), 496-502.
- 12 5. Lin, P.; Yan, F.; Chan, H. L., Ion-sensitive properties of organic electrochemical
13 transistors. *ACS Appl. Mater. Interfaces* **2010**, *2* (6), 1637-1641.
- 14 6. Kim, Y.; Lim, T.; Kim, C.-H.; Yeo, C. S.; Seo, K.; Kim, S.-M.; Kim, J.; Park, S.
15 Y.; Ju, S.; Yoon, M.-H., Organic electrochemical transistor-based channel dimension-
16 independent single-strand wearable sweat sensors. *NPG Asia Mater.* **2018**, *10* (11),
17 1086-1095.
- 18 7. Tao, W.; Lin, P.; Hu, J.; Ke, S.; Song, J.; Zeng, X., A sensitive DNA sensor based
19 on an organic electrochemical transistor using a peptide nucleic acid-modified
20 nanoporous gold gate electrode. *RSC Adv.* **2017**, *7* (82), 52118-52124.
- 21 8. Bihar, E.; Deng, Y.; Miyake, T.; Saadaoui, M.; Malliaras, G. G.; Rolandi, M., A
22 disposable paper breathalyzer with an alcohol sensing organic electrochemical
23 transistor. *Sci. Rep.* **2016**, *6* (1), 27582.
- 24 9. Tang, H.; Yan, F.; Lin, P.; Xu, J.; Chan, H. L., Highly sensitive glucose biosensors
25 based on organic electrochemical transistors using platinum gate electrodes modified
26 with enzyme and nanomaterials. *Adv. Funct. Mater.* **2011**, *21* (12), 2264-2272.
- 27 10. Rivnay, J.; Ramuz, M.; Leleux, P.; Hama, A.; Huerta, M.; Owens, R. M., Organic



- 1 electrochemical transistors for cell-based impedance sensing. *Appl. Phys. Lett.* **2015**,
2 *106* (4).
- 3 11. Lin, P.; Yan, F.; Yu, J.; Chan, H. L.; Yang, M., The application of organic
4 electrochemical transistors in cell-based biosensors. *Adv. Mater.* **2010**, *33* (22), 3655-
5 3660.
- 6 12. White, H. S.; Kittlesen, G. P.; Wrighton, M. S., Chemical derivatization of an array
7 of three gold microelectrodes with polypyrrole: fabrication of a molecule-based
8 transistor. *J. Am. Soc.* **1984**, *106* (18), 5375-5377.
- 9 13. Rivnay, J.; Leleux, P.; Ferro, M.; Sessolo, M.; Williamson, A.; Koutsouras, D. A.;
10 Khodagholy, D.; Ramuz, M.; Strakosas, X.; Owens, R. M., High-performance
11 transistors for bioelectronics through tuning of channel thickness. *Sci. Adv.* **2015**, *1* (4),
12 e1400251.
- 13 14. Wu, X.; Surendran, A.; Ko, J.; Filonik, O.; Herzig, E. M.; Müller-Buschbaum, P.;
14 Leong, W. L., Ionic-liquid doping enables high transconductance, fast response time,
15 and high ion sensitivity in organic electrochemical transistors. *Adv. Mater.* **2019**, *31*
16 (2), 1805544.
- 17 15. Wu, W.; Feng, K.; Wang, Y.; Wang, J.; Huang, E.; Li, Y.; Jeong, S. Y.; Woo, H.
18 Y.; Yang, K.; Guo, X., Selenophene Substitution Enabled High-Performance n-Type
19 Polymeric Mixed Ionic-Electronic Conductors for Organic Electrochemical Transistors
20 and Glucose Sensors. *Adv. Mater.* **2024**, *36* (1), 2310503.
- 21 16. Feng, K.; Shan, W.; Wang, J.; Lee, J. W.; Yang, W.; Wu, W.; Wang, Y.; Kim, B.
22 J.; Guo, X.; Guo, H., Cyano-Functionalized n-Type Polymer with High Electron
23 Mobility for High-Performance Organic Electrochemical Transistors. *Adv. Mater.* **2022**,
24 *34* (24), 2201340.
- 25 17. Kim, Y.; Noh, H.; Paulsen, B. D.; Kim, J.; Jo, I. Y.; Ahn, H.; Rivnay, J.; Yoon, M.
26 H., Strain-engineering induced anisotropic crystallite orientation and maximized carrier
27 mobility for high-performance microfiber-based organic bioelectronic devices. *Adv.*



- 1 *Mater.* **2021**, *33* (10), 2007550.
- 2 18. Kim, S.-M.; Kim, C.-H.; Kim, Y.; Kim, N.; Lee, W.-J.; Lee, E.-H.; Kim, D.; Park,
3 S.; Lee, K.; Rivnay, J., Influence of PEDOT: PSS crystallinity and composition on
4 electrochemical transistor performance and long-term stability. *Nat. Commun.* **2018**, *9*
5 (1), 3858.
- 6 19. Savva, A.; Hallani, R.; Cendra, C.; Surgailis, J.; Hidalgo, T. C.; Wustoni, S.;
7 Sheelamanthula, R.; Chen, X.; Kirkus, M.; Giovannitti, A., Balancing ionic and
8 electronic conduction for high-performance organic electrochemical transistors. *Adv.*
9 *Funct. Mater.* **2020**, *30* (11), 1907657.
- 10 20. Pitsalidis, C.; Pappa, A. M.; Porel, M.; Artim, C. M.; Faria, G. C.; Duong, D. D.;
11 Alabi, C. A.; Daniel, S.; Salleo, A.; Owens, R. M., Biomimetic electronic devices for
12 measuring bacterial membrane disruption. *Adv. Mater.* **2018**, *30* (39), 1803130.
- 13 21. Hütter, P. C.; Rothländer, T.; Haase, A.; Trimmel, G.; Stadlober, B., Influence of
14 geometry variations on the response of organic electrochemical transistors. *Appl. Phys.*
15 *Lett.* **2013**, *103* (4).
- 16 22. Bernards, D. A.; Malliaras, G. G., Steady-state and transient behavior of organic
17 electrochemical transistors. *Adv. Funct. Mater.* **2007**, *17* (17), 3538-3544.
- 18 23. Inal, S.; Malliaras, G. G.; Rivnay, J., Benchmarking organic mixed conductors for
19 transistors. *Nat. Commun.* **2017**, *8* (1), 1767.
- 20 24. Proctor, C. M.; Rivnay, J.; Malliaras, G. G., Understanding volumetric capacitance
21 in conducting polymers. In *J. Polym. Sci., Part B: Polym. Phys.*, Wiley Online Library:
22 2016; Vol. 54, pp 1433-1436.
- 23 25. Li, Y.; Zhang, S.; Li, X.; Unnava, V. R. N.; Cicoira, F., Highly stretchable PEDOT:
24 PSS organic electrochemical transistors achieved via polyethylene glycol addition.
25 *Flexible Printed Electron.* **2019**, *4* (4), 044004.
- 26 26. Dai, S.; Dai, Y.; Zhao, Z.; Xia, F.; Li, Y.; Liu, Y.; Cheng, P.; Strzalka, J.; Li, S.;
27 Li, N., Intrinsically stretchable neuromorphic devices for on-body processing of health



- 1 data with artificial intelligence. *Matter* **2022**, *5* (10), 3375-3390.
- 2 27. Parlak, O.; Keene, S. T.; Marais, A.; Curto, V. F.; Salleo, A., Molecularly selective
3 nanoporous membrane-based wearable organic electrochemical device for noninvasive
4 cortisol sensing. *Sci. Adv.* **2018**, *4* (7), eaar2904.
- 5 28. Andersson Ersman, P.; Lassnig, R.; Strandberg, J.; Tu, D.; Keshmiri, V.;
6 Forchheimer, R.; Fabiano, S.; Gustafsson, G.; Berggren, M., All-printed large-scale
7 integrated circuits based on organic electrochemical transistors. *Nat. Commun.* **2019**,
8 *10* (1), 5053.
- 9 29. Kayser, L. V.; Lipomi, D. J., Stretchable conductive polymers and composites
10 based on PEDOT and PEDOT: PSS. *Adv. Mater.* **2019**, *31* (10), 1806133.
- 11 30. Gualandi, I.; Marzocchi, M.; Achilli, A.; Cavedale, D.; Bonfiglio, A.; Fraboni, B.,
12 Textile organic electrochemical transistors as a platform for wearable biosensors. *Sci.*
13 *Rep.* **2016**, *6* (1), 33637.
- 14 31. Means, A. K.; Grunlan, M. A., Modern strategies to achieve tissue-mimetic,
15 mechanically robust hydrogels. In *ACS Macro Lett.*, ACS Publications: 2019.
- 16 32. Yuk, H.; Lu, B.; Zhao, X., Hydrogel bioelectronics. *Chem. Soc. Rev.* **2019**, *48* (6),
17 1642-1667.
- 18 33. Liu, X.; Liu, J.; Lin, S.; Zhao, X., Hydrogel machines. *Mater. Today* **2020**, *36*, 102-
19 124.
- 20 34. Bai, J.; Liu, D.; Tian, X.; Wang, Y.; Cui, B.; Yang, Y.; Dai, S.; Lin, W.; Zhu, J.;
21 Wang, J., Coin-sized, fully integrated, and minimally invasive continuous glucose
22 monitoring system based on organic electrochemical transistors. *Sci. Adv.* **2024**, *10* (16),
23 eadl1856.
- 24 35. Ko, J.; Wu, X.; Surendran, A.; Muhammad, B. T.; Leong, W. L., Self-healable
25 organic electrochemical transistor with high transconductance, fast response, and long-
26 term stability. *ACS Appl. Mater. Interfaces* **2020**, *12* (30), 33979-33988.
- 27 36. Han, S.; Yu, S.; Hu, S.; Chen, H.-j.; Wu, J.; Liu, C., A high endurance, temperature-



- 1 resilient, and robust organic electrochemical transistor for neuromorphic circuits. *J.*
2 *Mater. Chem. C* **2021**, *9* (35), 11801-11808.
- 3 37. Jo, Y. J.; Kwon, K. Y.; Khan, Z. U.; Crispin, X.; Kim, T.-i., Gelatin hydrogel-based
4 organic electrochemical transistors and their integrated logic circuits. *ACS Appl. Mater.*
5 *Interfaces* **2018**, *10* (45), 39083-39090.
- 6 38. Kim, C.-H.; Azimi, M.; Fan, J.; Nagarajan, H.; Wang, M.; Cicoira, F., All-printed
7 and stretchable organic electrochemical transistors using a hydrogel electrolyte.
8 *Nanoscale* **2023**, *15* (7), 3263-3272.
- 9 39. Sessolo, M.; Rivnay, J.; Bandiello, E.; Malliaras, G. G.; Bolink, H. J., Ion-selective
10 organic electrochemical transistors. *Adv. Mater.* **2014**, *26* (28), 4803-4807.
- 11 40. Berto, M.; Diacci, C.; Theuer, L.; Di Lauro, M.; Simon, D. T.; Berggren, M.;
12 Biscarini, F.; Beni, V.; Bortolotti, C. A., Label free urea biosensor based on organic
13 electrochemical transistors. *Flexible Printed Electron.* **2018**, *3* (2), 024001.
- 14 41. Galliani, M.; Diacci, C.; Berto, M.; Sensi, M.; Beni, V.; Berggren, M.; Borsari, M.;
15 Simon, D. T.; Biscarini, F.; Bortolotti, C. A., Flexible printed organic electrochemical
16 transistors for the detection of uric acid in artificial wound exudate. *Adv. Mater.*
17 *Interfaces* **2020**, *7* (23), 2001218.
- 18 42. Tseng, A. C.; Sakata, T., Direct electrochemical signaling in organic
19 electrochemical transistors comprising high-conductivity double-network hydrogels.
20 *ACS Appl. Mater. Interfaces* **2022**, *14* (21), 24729-24740.
- 21 43. Spyropoulos, G. D.; Gelinis, J. N.; Khodagholy, D., Internal ion-gated organic
22 electrochemical transistor: A building block for integrated bioelectronics. *Sci. Adv.*
23 **2019**, *5* (2), eaau7378.
- 24 44. Lee, H.; Lee, S.; Lee, W.; Yokota, T.; Fukuda, K.; Someya, T., Ultrathin organic
25 electrochemical transistor with nonvolatile and thin gel electrolyte for long-term
26 electrophysiological monitoring. *Adv. Funct. Mater.* **2019**, *29* (48), 1906982.
- 27 45. Correa, S.; Grosskopf, A. K.; Lopez Hernandez, H.; Chan, D.; Yu, A. C.; Stapleton,



- 1 L. M.; Appel, E. A., Translational applications of hydrogels. *Chem. Rev.* **2021**, *21* (18),
2 11385-11457.
- 3 46. Borem, R.; Madeline, A.; Walters, J.; Mayo, H.; Gill, S.; Mercuri, J., Angle-ply
4 biomaterial scaffold for annulus fibrosus repair replicates native tissue mechanical
5 properties, restores spinal kinematics, and supports cell viability. *Acta Biomater.* **2017**,
6 *58*, 254-268.
- 7 47. Zeng, Y.; Chen, C.; Liu, W.; Fu, Q.; Han, Z.; Li, Y.; Feng, S.; Li, X.; Qi, C.; Wu,
8 J., Injectable microcryogels reinforced alginate encapsulation of mesenchymal stromal
9 cells for leak-proof delivery and alleviation of canine disc degeneration. *Biomaterials*
10 **2015**, *59*, 53-65.
- 11 48. Yuk, H.; Wu, J.; Zhao, X., Hydrogel interfaces for merging humans and machines.
12 *Nat. Rev. Mater.* **2022**, *7* (12), 935-952.
- 13 49. Kim, Y.-T.; Hong, Y.-S.; Kimmel, R. M.; Rho, J.-H.; Lee, C.-H., New approach
14 for characterization of gelatin biopolymer films using proton behavior determined by
15 low field ¹H NMR spectrometry. *J. Agric. Food Chem.* **2007**, *55* (26), 10678-10684.
- 16 50. Silva, M.; Barbosa, P.; Rodrigues, L.; Gonçalves, A.; Costa, C.; Fortunato, E.,
17 Gelatin in electrochromic devices. *Opt. Mater* **2010**, *32* (6), 719-722.
- 18 51. Basu, T.; Middy, T.; Tarafdar, S., Ion-conductivity study and anomalous diffusion
19 analysis of plasticized gelatin films. *J. Appl. Polym. Sci.* **2013**, *130* (4), 3018-3024.
- 20 52. Nguyen-Dang, T.; Harrison, K.; Lill, A.; Dixon, A.; Lewis, E.; Vollbrecht, J.;
21 Hachisu, T.; Biswas, S.; Visell, Y.; Nguyen, T. Q., Biomaterial-Based Solid-Electrolyte
22 Organic Electrochemical Transistors for Electronic and Neuromorphic Applications.
23 *Adv. Electron. Mater.* **2021**, *7* (12), 2100519.
- 24 53. Zhong, Y.; Lopez-Larrea, N.; Alvarez-Tirado, M.; Casado, N.; Koklu, A.; Marks,
25 A.; Moser, M.; McCulloch, I.; Mecerreyes, D.; Inal, S., Eutectogels as a Semisolid
26 Electrolyte for Organic Electrochemical Transistors. *Chem. Mater.* **2024**.
- 27 54. Del Agua, I.; Porcarelli, L.; Curto, V.; Sanchez-Sanchez, A.; Ismailova, E.;



- 1 Malliaras, G.; Mecerreyes, D., A Na⁺ conducting hydrogel for protection of organic
2 electrochemical transistors. *J. Mater. Chem. B* **2018**, *6* (18), 2901-2906.
- 3 55. Khodagholy, D.; Curto, V. F.; Fraser, K. J.; Gurfinkel, M.; Byrne, R.; Diamond,
4 D.; Malliaras, G. G.; Benito-Lopez, F.; Owens, R. M., Organic electrochemical
5 transistor incorporating an ionogel as a solid state electrolyte for lactate sensing. *J.*
6 *Mater. Chem.* **2012**, *22* (10), 4440-4443.
- 7 56. Tseng, C. P.; Liu, F.; Zhang, X.; Huang, P. C.; Campbell, I.; Li, Y.; Atkinson, J.
8 T.; Terlier, T.; Ajo-Franklin, C. M.; Silberg, J. J., Solution-deposited and Patternable
9 conductive polymer thin-film electrodes for microbial bioelectronics. *Adv. Mater.* **2022**,
10 *34* (13), 2109442.
- 11 57. Welch, M. E.; Doublet, T.; Bernard, C.; Malliaras, G. G.; Ober, C. K., A glucose
12 sensor via stable immobilization of the GOx enzyme on an organic transistor using a
13 polymer brush. *J. Polym. Sci., Part A: Polym. Chem.* **2015**, *53* (2), 372-377.
- 14 58. Han, S.; Yu, S.; Hu, S.; Liang, X.; Luo, Y.; Liu, C., Ion transport to temperature
15 and gate in organic electrochemical transistors with anti-freezing hydrogel. *Org.*
16 *Electron.* **2022**, *108*, 106605.
- 17 59. Zhang, L.; Jiang, D.; Dong, T.; Das, R.; Pan, D.; Sun, C.; Wu, Z.; Zhang, Q.; Liu,
18 C.; Guo, Z., Overview of ionogels in flexible electronics. *Chem. Rec.* **2020**, *20* (9), 948-
19 967.
- 20 60. Ghorbanizamani, F.; Moulahoum, H.; Celik, E. G.; Timur, S., Ionic liquids
21 enhancement of hydrogels and impact on biosensing applications. *J. Mol. Liq.* **2022**,
22 *357*, 119075.
- 23 61. Wang, X.; Hao, J., Recent advances in ionic liquid-based electrochemical
24 biosensors. *Sci. Bull.* **2016**, *61* (16), 1281-1295.
- 25 62. Wang, D.; Zhao, S.; Yin, R.; Li, L.; Lou, Z.; Shen, G., Recent advanced
26 applications of ion-gel in ionic-gated transistor. *npj Flexible Electron.* **2021**, *5* (1), 13.
- 27 63. Gao, N.; Wu, X.; He, Y.; Ma, Q.; Wang, Y., Reconfigurable and recyclable circuits



- 1 based on liquid passive components. *Adv. Electron. Mater.* **2020**, *6* (8), 1901388.
- 2 64. He, R.; Lv, A.; Jiang, X.; Cai, C.; Wang, Y.; Yue, W.; Huang, L.; Yin, X. B.; Chi,
3 L., Organic Electrochemical Transistor Based on Hydrophobic Polymer Tuned by Ionic
4 Gels. *Angew. Chem., Int. Ed.* **2023**, *62* (37), e202304549.
- 5 65. Amoli, V.; Kim, J. S.; Kim, S. Y.; Koo, J.; Chung, Y. S.; Choi, H.; Kim, D. H.,
6 Ionic tactile sensors for emerging human-interactive technologies: a review of recent
7 progress. *Adv. Funct. Mater.* **2020**, *30* (20), 1904532.
- 8 66. Li, R.; Wang, L.; Kong, D.; Yin, L., Recent progress on biodegradable materials
9 and transient electronics. *Bioact. Mater.* **2018**, *3* (3), 322-333.
- 10 67. Zhao, Y.; Haseena, S.; Ravva, M. K.; Zhang, S.; Li, X.; Jiang, J.; Fu, Y.; Inal, S.;
11 Wang, Q.; Wang, Y., Side chain engineering enhances the high-temperature resilience
12 and ambient stability of organic synaptic transistors for neuromorphic applications.
13 *Nano Energy* **2022**, *104*, 107985.
- 14 68. Luque, G. C.; Picchio, M. L.; Martins, A. P.; Dominguez-Alfaro, A.; Ramos, N.;
15 del Agua, I.; Marchiori, B.; Mecerreyes, D.; Minari, R. J.; Tomé, L. C., 3D printable
16 and biocompatible ion gels for body sensor applications. *Adv. Electron. Mater.* **2021**, *7*
17 (8), 2100178.
- 18 69. Isik, M.; Lonjaret, T.; Sardon, H.; Marcilla, R.; Herve, T.; Malliaras, G. G.;
19 Ismailova, E.; Mecerreyes, D., Cholinium-based ion gels as solid electrolytes for long-
20 term cutaneous electrophysiology. *J. Mater. Chem. C* **2015**, *3* (34), 8942-8948.
- 21 70. Wang, H.; Wang, Z.; Yang, J.; Xu, C.; Zhang, Q.; Peng, Z., Ionic gels and their
22 applications in stretchable electronics. *Macromol. Rapid Commun.* **2018**, *39* (16),
23 1800246.
- 24 71. Lodge, T. P.; Ueki, T., Mechanically tunable, readily processable ion gels by self-
25 assembly of block copolymers in ionic liquids. *Acc. Chem. Res.* **2016**, *49* (10), 2107-
26 2114.
- 27 72. Hong, Y.; Lin, Z.; Yang, Y.; Jiang, T.; Shang, J.; Luo, Z., Biocompatible



- 1 conductive hydrogels: applications in the field of biomedicine. *Int. J. Mol. Ser.* **2022**,
2 *23* (9), 4578.
- 3 73. Zhao, F.; Shi, Y.; Pan, L.; Yu, G., Multifunctional nanostructured conductive
4 polymer gels: synthesis, properties, and applications. *Acc. Chem. Res.* **2017**, *50* (7),
5 1734-1743.
- 6 74. Wang, Y.; Zhu, C.; Pfattner, R.; Yan, H.; Jin, L.; Chen, S.; Molina-Lopez, F.; Lissel,
7 F.; Liu, J.; Rabiah, N. I., A highly stretchable, transparent, and conductive polymer.
8 *Sci. Adv.* **2017**, *3* (3), e1602076.
- 9 75. Nawaz, A.; Liu, Q.; Leong, W. L.; Fairfull-Smith, K. E.; Sonar, P., Organic
10 electrochemical transistors for in vivo bioelectronics. *Adv. Mater.* **2021**, *33* (49),
11 2101874.
- 12 76. Inal, S.; Rivnay, J.; Suiu, A.-O.; Malliaras, G. G.; McCulloch, I., Conjugated
13 polymers in bioelectronics. *Acc. Chem. Res.* **2018**, *51* (6), 1368-1376.
- 14 77. Kavanagh, A.; Byrne, R.; Diamond, D.; Fraser, K. J., Stimuli responsive ionogels
15 for sensing applications—an overview. *Membranes* **2012**, *2* (1), 16-39.
- 16 78. Wu, X.; Chen, S.; Moser, M.; Moudgil, A.; Griggs, S.; Marks, A.; Li, T.;
17 McCulloch, I.; Leong, W. L., High Performing Solid-State Organic Electrochemical
18 Transistors Enabled by Glycolated Polythiophene and Ion-Gel Electrolyte with a Wide
19 Operation Temperature Range from– 50 to 110° C. *Adv. Funct. Mater.* **2023**, *33* (3),
20 2209354.
- 21 79. Zhang, S.; Cicoira, F., Water-enabled healing of conducting polymer films. *Adv.*
22 *Mater.* **2017**, *29* (40), 1703098.
- 23 80. Perera, M. M.; Ayres, N., Dynamic covalent bonds in self-healing, shape memory,
24 and controllable stiffness hydrogels. *Polym. Chem.* **2020**, *11* (8), 1410-1423.
- 25 81. Gong, Z.; Zhang, G.; Zeng, X.; Li, J.; Li, G.; Huang, W.; Sun, R.; Wong, C., High-
26 strength, tough, fatigue resistant, and self-healing hydrogel based on dual physically
27 cross-linked network. *ACS Appl. Mater. Interfaces* **2016**, *8* (36), 24030-24037.



- 1 82. Cai, C.; Zhang, X.; Li, Y.; Liu, X.; Wang, S.; Lu, M.; Yan, X.; Deng, L.; Liu, S.;
2 Wang, F., Self-healing hydrogel embodied with macrophage-regulation and
3 responsive-gene-silencing properties for synergistic prevention of peritendinous
4 adhesion. *Adv. Mater.* **2022**, *34* (5), 2106564.
- 5 83. Zhu, Z.; Lu, D.; Zhu, M.; Zhang, P.; Xiang, X., Smart Organogels with
6 Antiswelling, Strong Adhesion, and Freeze-Tolerance for Multi-Environmental
7 Wearable Bioelectronic Devices. *Chem. Mater.* **2024**.
- 8 84. Yao, X.; Zhang, S.; Qian, L.; Wei, N.; Nica, V.; Coseri, S.; Han, F., Super
9 stretchable, self-healing, adhesive ionic conductive hydrogels based on tailor-made
10 ionic liquid for high-performance strain sensors. *Adv. Funct. Mater.* **2022**, *32* (33),
11 2204565.
- 12 85. Li, P.; Zong, H.; Li, G.; Shi, Z.; Yu, X.; Zhang, K.; Xia, P.; Yan, S.; Yin, J.,
13 Building a Poly (amino acid)/Chitosan-Based Self-Healing Hydrogel via Host–Guest
14 Interaction for Cartilage Regeneration. *ACS Biomater. Sci. Eng.* **2023**, *9* (8), 4855-4866.
- 15 86. Tuncaboylu, D. C.; Sari, M.; Oppermann, W.; Okay, O., Tough and self-healing
16 hydrogels formed via hydrophobic interactions. *Macromolecules* **2011**, *44* (12), 4997-
17 5005.
- 18 87. Lu, D.; Lian, Q.; Zhu, M., Bioinspired Multistimuli-Induced Synergistic Changes
19 in Color and Shape of Hydrogel and Actuator Based on Fluorescent Microgels. *Adv.*
20 *Sci.* **2024**, *11* (3), 2304776.
- 21 88. Nakahata, M.; Takashima, Y.; Yamaguchi, H.; Harada, A., Redox-responsive self-
22 healing materials formed from host–guest polymers. *Nat. Commun.* **2011**, *2* (1), 511.
- 23 89. Lu, D.; Zhu, M.; Jin, J.; Saunders, B. R., Triply-responsive OEG-based microgels
24 and hydrogels: regulation of swelling ratio, volume phase transition temperatures and
25 mechanical properties. *Polym. Chem.* **2021**, *12* (30), 4406-4417.
- 26 90. Thornton, P. D.; Mart, R. J.; Ulijn, R. V., Enzyme-responsive polymer hydrogel
27 particles for controlled release. *Adv. Mater.* **2007**, *19* (9), 1252-1256.



- 1 91. Basu, P.; Saha, N.; Saha, T.; Saha, P., Polymeric hydrogel based systems for
2 vaccine delivery: A review. *Polymer* **2021**, *230*, 124088.
- 3 92. Lu, D.; Zhu, M.; Wu, S.; Lian, Q.; Wang, W.; Adlam, D.; Hoyland, J. A.; Saunders,
4 B. R., Programmed multiresponsive hydrogel assemblies with light-tunable mechanical
5 properties, actuation, and fluorescence. *Adv. Funct. Mater.* **2020**, *30* (11), 1909359.
- 6 93. Lu, D.; Zhu, M.; Li, X.; Zhu, Z.; Lin, X.; Guo, C. F.; Xiang, X., Thermosensitive
7 hydrogel-based, high performance flexible sensors for multi-functional e-skins. *J.*
8 *Mater. Chem. A* **2023**, *11* (34), 18247-18261.
- 9 94. Li, Z.; Li, Y.; Chen, C.; Cheng, Y., Magnetic-responsive hydrogels: From strategic
10 design to biomedical applications. *J. Controlled Release* **2021**, *335*, 541-556.
- 11 95. Kim, S. J.; Park, S. J.; Kim, I. Y.; Shin, M. S.; Kim, S. I., Electric stimuli responses
12 to poly (vinyl alcohol)/chitosan interpenetrating polymer network hydrogel in NaCl
13 solutions. *J. Appl. Polym. Sci.* **2002**, *86* (9), 2285-2289.
- 14 96. Zhou, Y.; Liu, G.; Guo, S., Advances in ultrasound-responsive hydrogels for
15 biomedical applications. *J. Mater. Chem. B* **2022**, *10* (21), 3947-3958.
- 16 97. Li, J.; Mooney, D. J., Designing hydrogels for controlled drug delivery. *Nat. Rev.*
17 *Mater.* **2016**, *1* (12), 1-17.
- 18 98. Yue, S.; He, H.; Li, B.; Hou, T., Hydrogel as a biomaterial for bone tissue
19 engineering: A review. *J. Nanomater.* **2020**, *10* (8), 1511.
- 20 99. Lenz, J.; Del Giudice, F.; Geisenhof, F. R.; Winterer, F.; Weitz, R. T., Vertical,
21 electrolyte-gated organic transistors show continuous operation in the MA cm⁻²
22 regime and artificial synaptic behaviour. *Nat. Nanotechnol.* **2019**, *14* (6), 579-585.
- 23 100. Kushida, S.; Smarsly, E.; Yoshinaga, K.; Wacker, I.; Yamamoto, Y.; Schröder,
24 R. R.; Bunz, U. H., Fast Response Organic Supramolecular Transistors Utilizing In-Situ
25 π -Ion Gels. *Adv. Mater.* **2021**, *33* (4), 2006061.
- 26 101. Fu, Y.; Kong, L.-a.; Chen, Y.; Wang, J.; Qian, C.; Yuan, Y.; Sun, J.; Gao, Y.;
27 Wan, Q., Flexible neuromorphic architectures based on self-supported multiterminal



- 1 organic transistors. *ACS Appl. Mater. Interfaces* **2018**, *10* (31), 26443-26450. DOI: 10.1039/D4TA05288A
- 2 102. Liu, Q.; Liu, Y.; Li, J.; Lau, C.; Wu, F.; Zhang, A.; Li, Z.; Chen, M.; Fu, H.;
3 Draper, J., Fully printed all-solid-state organic flexible artificial synapse for
4 neuromorphic computing. *ACS Appl. Mater. Interfaces* **2019**, *11* (18), 16749-16757.
- 5 103. Zhao, Y.; Song, S.; Ren, X.; Zhang, J.; Lin, Q.; Zhao, Y., Supramolecular
6 adhesive hydrogels for tissue engineering applications. *Chem. Rev.* **2022**, *122* (6), 5604-
7 5640.
- 8 104. Zhang, Y.; Chen, Q.; Dai, Z.; Dai, Y.; Xia, F.; Zhang, X., Nanocomposite
9 adhesive hydrogels: from design to application. *J. Mater. Chem. B* **2021**, *9* (3), 585-
10 593.
- 11 105. Li, S.; Cong, Y.; Fu, J., Tissue adhesive hydrogel bioelectronics. *J. Mater.*
12 *Chem. B* **2021**, *9* (22), 4423-4443.
- 13 106. Di, X.; Kang, Y.; Li, F.; Yao, R.; Chen, Q.; Hang, C.; Xu, Y.; Wang, Y.; Sun,
14 P.; Wu, G., Poly (N-isopropylacrylamide)/polydopamine/clay nanocomposite
15 hydrogels with stretchability, conductivity, and dual light-and thermo-responsive
16 bending and adhesive properties. *Colloids Surf., B* **2019**, *177*, 149-159.
- 17 107. Lu, Q.; Oh, D. X.; Lee, Y.; Jho, Y.; Hwang, D. S.; Zeng, H., Nanomechanics
18 of cation- π interactions in aqueous solution. *Angew. Chem., Int. Ed.* **2013**, *125* (14),
19 4036-4040.
- 20 108. Cea, C.; Spyropoulos, G. D.; Jastrzebska-Perfect, P.; Ferrero, J. J.; Gelinas, J.
21 N.; Khodagholy, D., Enhancement-mode ion-based transistor as a comprehensive
22 interface and real-time processing unit for in vivo electrophysiology. *Nat. Mater.* **2020**,
23 *19* (6), 679-686.
- 24 109. Guo, K.; Wustoni, S.; Koklu, A.; Díaz-Galicia, E.; Moser, M.; Hama, A.;
25 Alqahtani, A. A.; Ahmad, A. N.; Alhamlan, F. S.; Shuaib, M., Rapid single-molecule
26 detection of COVID-19 and MERS antigens via nanobody-functionalized organic
27 electrochemical transistors. *Nat. Biomed. Eng.* **2021**, *5* (7), 666-677.



- 1 110. Li, N.; Li, Y.; Cheng, Z.; Liu, Y.; Dai, Y.; Kang, S.; Li, S.; Shan, N.; Wang, S.;
2 Ziaja, A., Bioadhesive polymer semiconductors and transistors for intimate
3 biointerfaces. *Science* **2023**, *381* (6658), 686-693.
- 4 111. Rivnay, J.; Wang, H.; Fenno, L.; Deisseroth, K.; Malliaras, G. G., Next-
5 generation probes, particles, and proteins for neural interfacing. *Sci. Adv.* **2017**, *3* (6),
6 e1601649.
- 7 112. Fan, X.; Xu, B.; Liu, S.; Cui, C.; Wang, J.; Yan, F., Transfer-printed PEDOT:
8 PSS electrodes using mild acids for high conductivity and improved stability with
9 application to flexible organic solar cells. *ACS Appl. Mater. Interfaces* **2016**, *8* (22),
10 14029-14036.
- 11 113. Sekitani, T.; Someya, T., Stretchable, large-area organic electronics. *Adv.*
12 *Mater.* **2010**, *22* (20), 2228-2246.
- 13 114. Zhang, S.; Ling, H.; Chen, Y.; Cui, Q.; Ni, J.; Wang, X.; Hartel, M. C.; Meng,
14 X.; Lee, K.; Lee, J., Hydrogel-enabled transfer-printing of conducting polymer films
15 for soft organic bioelectronics. *Adv. Funct. Mater.* **2020**, *30* (6), 1906016.
- 16 115. Wang, M.; Luo, Y.; Wang, T.; Wan, C.; Pan, L.; Pan, S.; He, K.; Neo, A.;
17 Chen, X., Artificial skin perception. *Adv. Mater.* **2021**, *33* (19), 2003014.
- 18 116. Fan, X.; Nie, W.; Tsai, H.; Wang, N.; Huang, H.; Cheng, Y.; Wen, R.; Ma, L.;
19 Yan, F.; Xia, Y., PEDOT: PSS for flexible and stretchable electronics: modifications,
20 strategies, and applications. *Adv. Sci.* **2019**, *6* (19), 1900813.
- 21 117. Kim, D.-H.; Lu, N.; Ma, R.; Kim, Y.-S.; Kim, R.-H.; Wang, S.; Wu, J.; Won,
22 S. M.; Tao, H.; Islam, A., Epidermal electronics. *Science* **2011**, *333* (6044), 838-843.
- 23 118. Li, Y.; Wang, N.; Yang, A.; Ling, H.; Yan, F., Biomimicking stretchable
24 organic electrochemical transistor. *Adv. Electron. Mater.* **2019**, *5* (10), 1900566.
- 25 119. Dai, Y.; Dai, S.; Li, N.; Li, Y.; Moser, M.; Strzalka, J.; Prominski, A.; Liu, Y.;
26 Zhang, Q.; Li, S., Stretchable redox-active semiconducting polymers for
27 high-performance organic electrochemical transistors. *Adv. Mater.* **2022**, *34* (23),



- 1 2201178.
- 2 120. Fang, Y.; Yang, X.; Lin, Y.; Shi, J.; Prominski, A.; Clayton, C.; Ostroff, E.;
3 Tian, B., Dissecting biological and synthetic soft–hard interfaces for tissue-like systems.
4 *Chem. Rev.* **2021**, *122* (5), 5233-5276.
- 5 121. Minev, I. R.; Musienko, P.; Hirsch, A.; Barraud, Q.; Wenger, N.; Moraud, E.
6 M.; Gandar, J.; Capogrosso, M.; Milekovic, T.; Asboth, L., Electronic dura mater for
7 long-term multimodal neural interfaces. *Science* **2015**, *347* (6218), 159-163.
- 8 122. Gu, P.; Lu, L.; Yang, X.; Hu, Z.; Zhang, X.; Sun, Z.; Liang, X.; Liu, M.; Sun,
9 Q.; Huang, J., Highly Stretchable Semiconducting Aerogel Films for
10 High-Performance Flexible Electronics. *Adv. Funct. Mater.* **2024**, 2400589.
- 11 123. Doris, S. E.; Pierre, A.; Street, R. A., Dynamic and tunable threshold voltage
12 in organic electrochemical transistors. *Adv. Mater.* **2018**, *30* (15), 1706757.
- 13 124. Bernards, D. A.; Macaya, D. J.; Nikolou, M.; DeFranco, J. A.; Takamatsu, S.;
14 Malliaras, G. G., Enzymatic sensing with organic electrochemical transistors. *J. Mater.*
15 *Chem.* **2008**, *18* (1), 116-120.
- 16 125. Gualandi, I.; Tonelli, D.; Mariani, F.; Scavetta, E.; Marzocchi, M.; Fraboni,
17 B., Selective detection of dopamine with an all PEDOT: PSS organic electrochemical
18 transistor. *Sci. Rep.*: 2016; Vol. 6, p 35419.
- 19 126. Ghittorelli, M.; Lingstedt, L.; Romele, P.; Crăciun, N. I.; Kovács-Vajna, Z. M.;
20 Blom, P. W.; Torricelli, F., High-sensitivity ion detection at low voltages with current-
21 driven organic electrochemical transistors. *Nat. Commun.* **2018**, *9* (1), 1441.
- 22 127. Majak, D.; Fan, J.; Gupta, M., Fully 3D printed OECT based logic gate for
23 detection of cation type and concentration. *Sens. Actuators, B* **2019**, *286*, 111-118.
- 24 128. Koutsouras, D. A.; Lieberth, K.; Torricelli, F.; Gkoupidenis, P.; Blom, P. W.,
25 Selective ion detection with integrated organic electrochemical transistors. *Adv. Mater.*
26 *Technol.* **2021**, *6* (12), 2100591.
- 27 129. Liao, C.; Mak, C.; Zhang, M.; Chan, H. L.; Yan, F., Flexible organic



- 1 electrochemical transistors for highly selective enzyme biosensors and used for saliva
2 testing. *Adv. Mater.* **2015**, *27* (4), 676-681.
- 3 130. Demuru, S.; Kim, J.; El Chazli, M.; Bruce, S.; Dupertuis, M.; Binz, P.-A.;
4 Saubade, M.; Lafaye, C.; Briand, D., Antibody-coated wearable organic
5 electrochemical transistors for cortisol detection in human sweat. *ACS Sens.* **2022**, *7*
6 (9), 2721-2731.
- 7 131. Macchia, E.; Ghittorelli, M.; Torricelli, F.; Torsi, L. In *Organic*
8 *electrochemical transistor immuno-sensor operating at the femto-molar limit of*
9 *detection*, IEEE International Workshop on Advances in Sensors and Interfaces, IEEE:
10 2017; pp 68-72.
- 11 132. Fan, J.; Pico, A. A. F.; Gupta, M., A functionalization study of aerosol jet
12 printed organic electrochemical transistors (OECTs) for glucose detection. *Mater. Adv.*
13 **2021**, *2* (22), 7445-7455.
- 14 133. Nair, R. R., Glucose sensing and hybrid instrumentation based on printed
15 organic electrochemical transistors. *Flexible Printed Electron.* **2020**, *5* (1), 015001.
- 16 134. Druet, V.; Nayak, P. D.; Koklu, A.; Ohayon, D.; Hama, A.; Chen, X.; Moser,
17 M.; McCulloch, I.; Inal, S., Operation mechanism of n-type organic electronic
18 metabolite sensors. *Adv. Electron. Mater.* **2022**, *8* (10), 2200065.
- 19 135. Zhou, Z.; Wu, X.; Tam, T. L. D.; Tang, C. G.; Chen, S.; Hou, K.; Li, T.; He,
20 Q.; Sit, J. J.; Xu, J., Highly Stable Ladder-Type Conjugated Polymer Based Organic
21 Electrochemical Transistors for Low Power and Signal Processing-Free Surface
22 Electromyogram Triggered Robotic Hand Control. *Adv. Funct. Mater.* **2024**, *34* (1),
23 2305780.
- 24 136. Tyrrell, J. E.; Petkos, K.; Drakakis, E. M.; Boutelle, M. G.; Campbell, A. J.,
25 Organic Electrochemical Transistor Common-Source Amplifier for
26 Electrophysiological Measurements. *Adv. Funct. Mater.* **2021**, *31* (33), 2103385.
- 27 137. Yang, A.; Song, J.; Liu, H.; Zhao, Z.; Li, L.; Yan, F., Wearable Organic



- 1 Electrochemical Transistor Array for Skin-Surface Electrocardiogram Mapping Above
2 a Human Heart. *Adv. Funct. Mater.* **2023**, *33* (17), 2215037.
- 3 138. Andersen, S. S.; Jackson, A. D.; Heimbürg, T., Towards a thermodynamic
4 theory of nerve pulse propagation. *Prog. Neurobiol.* **2009**, *88* (2), 104-113.
- 5 139. Singh, S.; Dodt, J.; Volkers, P.; Hethershaw, E.; Philippou, H.; Ivaskevicius,
6 V.; Imhof, D.; Oldenburg, J.; Biswas, A., Structure functional insights into calcium
7 binding during the activation of coagulation factor XIII A. *Sci. Rep.* **2019**, *9* (1), 11324.
- 8 140. He, F. J.; MacGregor, G. A., A comprehensive review on salt and health and
9 current experience of worldwide salt reduction programmes. *J. Hum. Hypertens.* **2009**,
10 *23* (6), 363-384.
- 11 141. Giridharagopal, R.; Flagg, L.; Harrison, J.; Ziffer, M.; Onorato, J.; Luscombe,
12 C.; Ginger, D., Electrochemical strain microscopy probes morphology-induced
13 variations in ion uptake and performance in organic electrochemical transistors. *Nat.*
14 *Mater.* **2017**, *16* (7), 737-742.
- 15 142. Szigeti, Z.; Vigassy, T.; Bakker, E.; Pretsch, E., Approaches to improving the
16 lower detection limit of polymeric membrane ion-selective electrodes. *Electroanalysis*
17 **2006**, *18* (13-14), 1254-1265.
- 18 143. Keene, S. T.; Fogarty, D.; Cooke, R.; Casadevall, C. D.; Salleo, A.; Parlak, O.,
19 Wearable organic electrochemical transistor patch for multiplexed sensing of calcium
20 and ammonium ions from human perspiration. *Adv. Healthcare Mater.* **2019**, *8* (24),
21 1901321.
- 22 144. Mousavi, Z.; Ekholm, A.; Bobacka, J.; Ivaska, A., Ion-selective organic
23 electrochemical junction transistors based on poly (3, 4-ethylenedioxythiophene) doped
24 with poly (styrene sulfonate). *Electroanalysis* **2009**, *21* (3-5), 472-479.
- 25 145. Liao, J.; Si, H.; Zhang, X.; Lin, S., Functional sensing interfaces of PEDOT:
26 PSS organic electrochemical transistors for chemical and biological sensors: a mini
27 review. *Sensors* **2019**, *19* (2), 218.



- 1 146. Tang, H.; Lin, P.; Chan, H. L.; Yan, F., Highly sensitive dopamine biosensors
2 based on organic electrochemical transistors. *Biosens. Bioelectron.* **2011**, *26* (11),
3 4559-4563.
- 4 147. Gualandi, I.; Marzocchi, M.; Scavetta, E.; Calienni, M.; Bonfiglio, A.; Fraboni,
5 B., A simple all-PEDOT: PSS electrochemical transistor for ascorbic acid sensing. *J.*
6 *Mater. Chem. B* **2015**, *3* (33), 6753-6762.
- 7 148. Arcangeli, D.; Gualandi, I.; Mariani, F.; Tessarolo, M.; Ceccardi, F.; Decataldo,
8 F.; Melandri, F.; Tonelli, D.; Fraboni, B.; Scavetta, E., Smart bandaid integrated with
9 fully textile OECT for uric acid real-time monitoring in wound exudate. *ACS Sens.*
10 **2023**, *8* (4), 1593-1608.
- 11 149. Xi, X.; Wu, D.; Ji, W.; Zhang, S.; Tang, W.; Su, Y.; Guo, X.; Liu, R.,
12 Manipulating the sensitivity and selectivity of OECT-based biosensors via the surface
13 engineering of carbon cloth gate electrodes. *Adv. Funct. Mater.* **2020**, *30* (4), 1905361.
- 14 150. Ma, X.; Chen, H.; Zhang, P.; Hartel, M. C.; Cao, X.; Diltemiz, S. E.; Zhang,
15 Q.; Iqbal, J.; de Barros, N. R.; Liu, L., OFET and OECT, two types of Organic Thin-
16 Film Transistor used in glucose and DNA biosensors: A Review. *IEEE Sens. J.* **2022**,
17 *22* (12), 11405-11414.
- 18 151. Liao, C.; Zhang, M.; Niu, L.; Zheng, Z.; Yan, F., Highly selective and sensitive
19 glucose sensors based on organic electrochemical transistors with graphene-modified
20 gate electrodes. *J. Mater. Chem. B* **2013**, *1* (31), 3820-3829.
- 21 152. Currano, L. J.; Sage, F. C.; Hagedon, M.; Hamilton, L.; Patrone, J.;
22 Gerasopoulos, K., Wearable sensor system for detection of lactate in sweat. *Sci. Rep.*
23 **2018**, *8* (1), 1-11.
- 24 153. Lafuente, J.-L.; González, S.; Aibar, C.; Rivera, D.; Avilés, E.; Beunza, J.-J.,
25 Continuous and Non-Invasive Lactate Monitoring Techniques in Critical Care Patients.
26 *Biosensors* **2024**, *14* (3), 148.
- 27 154. Ok, J.; Park, S.; Jung, Y. H.; Kim, T. i., Wearable and Implantable



- 1 Cortisol-Sensing Electronics for Stress Monitoring. *Adv. Mater.* **2024**, *36* (1), 2211595.
- 2 155. Zhang, L.; Wang, G.; Xiong, C.; Zheng, L.; He, J.; Ding, Y.; Lu, H.; Zhang,
3 G.; Cho, K.; Qiu, L., Chirality detection of amino acid enantiomers by organic
4 electrochemical transistor. *J. Biosens. Bioelectron.* **2018**, *105*, 121-128.
- 5 156. Dhawan, G.; Sumana, G.; Malhotra, B., Recent developments in urea
6 biosensors. *Biochem. Eng. J.* **2009**, *44* (1), 42-52.
- 7 157. Cirillo, P.; Sato, W.; Reungjui, S.; Heinig, M.; Gersch, M.; Sautin, Y.;
8 Nakagawa, T.; Johnson, R. J., Uric acid, the metabolic syndrome, and renal disease. *J.*
9 *Am. Soc. Nephrol.* **2006**, *17* (12_suppl_3), S165-S168.
- 10 158. Howard, S. C.; Pui, C.-H.; Ribeiro, R. C., Tumor lysis syndrome. *Renal*
11 *Disease in Cancer Patients* **2014**, 39-64.
- 12 159. Heinig, M.; Johnson, R. J., Role of uric acid in hypertension, renal disease, and
13 metabolic syndrome. *Cleveland Clin. Q.* **2006**, *73* (12), 1059.
- 14 160. Gilletti, A.; Muthuswamy, J., Brain micromotion around implants in the rodent
15 somatosensory cortex. *J. Neural Eng.* **2006**, *3* (3), 189.
- 16 161. Schmatz, B.; Lang, A. W.; Reynolds, J. R., Fully printed organic
17 electrochemical transistors from green solvents. *Adv. Funct. Mater.* **2019**, *29* (44),
18 1905266.
- 19 162. Afonso, M.; Morgado, J.; Alcácer, L., Inkjet printed organic electrochemical
20 transistors with highly conducting polymer electrolytes. *J. Appl. Phys.* **2016**, *120* (16).
- 21 163. Ye, T.; Wang, J.; Jiao, Y.; Li, L.; He, E.; Wang, L.; Li, Y.; Yun, Y.; Li, D.;
22 Lu, J., A tissue-like soft all-hydrogel battery. *Adv. Mater.* **2022**, *34* (4), 2105120.
- 23 164. Yang, P.; Yang, J.-L.; Liu, K.; Fan, H. J., Hydrogels enable future smart
24 batteries. *ACS Nano* **2022**, *16* (10), 15528-15536.
- 25 165. Huang, S.; Hou, L.; Li, T.; Jiao, Y.; Wu, P., Antifreezing hydrogel electrolyte
26 with ternary hydrogen bonding for high-performance zinc-ion batteries. *Adv. Mater.*
27 **2022**, *34* (14), 2110140.



- 1 166. Khazaeli, A.; Godbille-Cardona, G.; Barz, D. P., A Novel Flexible Hybrid
2 Battery–Supercapacitor Based on a Self-Assembled Vanadium-Graphene Hydrogel.
3 *Adv. Funct. Mater.* **2020**, *30* (21), 1910738.
- 4 167. Chen, Z.; To, J. W.; Wang, C.; Lu, Z.; Liu, N.; Chortos, A.; Pan, L.; Wei, F.;
5 Cui, Y.; Bao, Z., A three-dimensionally interconnected carbon nanotube–conducting
6 polymer hydrogel network for high-performance flexible battery electrodes. *Adv.*
7 *Energy Mater.* **2014**, *4* (12), 1400207.
- 8 168. Jiang, D.; Lu, N.; Li, L.; Zhang, H.; Luan, J.; Wang, G., A highly compressible
9 hydrogel electrolyte for flexible Zn-MnO₂ battery. *J. Colloid Interface Sci.* **2022**, *608*,
10 1619-1626.
- 11 169. Li, L.; Fang, B.; Ren, D.; Fu, L.; Zhou, Y.; Yang, C.; Zhang, F.; Feng, X.;
12 Wang, L.; He, X., Thermal-switchable, trifunctional ceramic–hydrogel nanocomposites
13 enable full-lifecycle security in practical battery systems. *ACS Nano* **2022**, *16* (7),
14 10729-10741.
15



1 **Biographies**

2

3 **Dongdong Lu** obtained her and PhD degree (2020) in Polymer Science and
4 Engineering from the university of manchester (UOM), United Kingdom. She worked
5 as a postdoc in Material Science and Engineering at Southern University of Science and
6 Technology (SUST) from 2020 to 2022. Now she is a Researcher of School of Physical
7 Sciences at Great Bay University (GBU). Her current research focuses on design,
8 synthesis and fabrication of multi-functional polymers, nanomaterials, microgels and
9 hydrogels used in fluorescent sensorand flexible electronics.



10

11 **Hu Chen** is a principal investigator at Great Bay University in China from 2022. He
12 obtained his PhD from Peking University and received intensive training in organic
13 synthesis in 2014. He subsequently joined Professor Iain McCulloch's group to focus
14 on organic electronics. His current research centers on designing and synthesizing high-
15 performance innovative organic semiconductors as well as device fabrication and
16 characterization.



Data Availability Statement

View Article Online
DOI: 10.1039/D4TA05288A

Data availability is not applicable to this article as no new data were created or analyzed in this study.

